

# Distributionally Robust Multi-objective Bayesian Optimization under Uncertain Environments

Yu Inatsu<sup>1,\*</sup> Ichiro Takeuchi<sup>2,3</sup>

<sup>1</sup> Department of Computer Science, Nagoya Institute of Technology

<sup>2</sup> Department of Mechanical Systems Engineering, Nagoya University

<sup>3</sup> RIKEN Center for Advanced Intelligence Project

\* E-mail: inatsu.yu@nitech.ac.jp

## ABSTRACT

In this study, we address the problem of optimizing multi-output black-box functions under uncertain environments. We formulate this problem as the estimation of the uncertain Pareto-frontier (PF) of a multi-output Bayesian surrogate model with two types of variables: *design variables* and *environmental variables*. We consider this problem within the context of Bayesian optimization (BO) under uncertain environments, where the design variables are controllable, whereas the environmental variables are assumed to be random and not controllable. The challenge of this problem is to robustly estimate the PF when the distribution of the environmental variables is unknown, that is, to estimate the PF when the environmental variables are generated from the worst possible distribution. We propose a method for solving the BO problem by appropriately incorporating the uncertainties of the environmental variables and their probability distribution. We demonstrate that the proposed method can find an arbitrarily accurate PF with high probability in a finite number of iterations. We also evaluate the performance of the proposed method through numerical experiments.

## 1. Introduction

In many industrial applications, we encounter the problem of optimizing the multi-output black-box function under uncertain environments. For example, in the problem of optimizing growing conditions for crops, we want to optimize several conditions such as fertilizer levels to maximize crop quality and yield under an uncertain environment such as weather conditions.

To formulate this problem, let  $f^{(1)}(\mathbf{x}, \mathbf{w})$  and  $f^{(2)}(\mathbf{x}, \mathbf{w})$  be a pair of outputs of a black-box function that we want to simultaneously maximize, where  $\mathbf{x} \in \mathcal{X}$  and  $\mathbf{w} \in \Omega$  are the *design variables* (such as fertilizer levels) and *environmental variables* (such as weather conditions) defined in domains  $\mathcal{X}$  and  $\Omega$ , respectively, where the former is controllable and the latter is not. To characterize the uncertainty of the environmental variables  $\mathbf{w}$ , we assume that it is sampled from an unknown probability distribution,  $P^\dagger$ . Because we do not know  $P^\dagger$ , we consider the case where we know only  $\mathcal{A}$ , which is a family of candidate distributions for  $\mathbf{w}$ .

This study aims to identify a *distributionally robust Pareto-frontier (DR-PF)* in the above setting, which is formulated as a PF of the following two functions:

$$F^{(1)}(\mathbf{x}) = \inf_{p(\mathbf{w}) \in \mathcal{A}} \int_{\Omega} f^{(1)}(\mathbf{x}, \mathbf{w}) p(\mathbf{w}) d\mathbf{w},$$
$$F^{(2)}(\mathbf{x}) = \inf_{p(\mathbf{w}) \in \mathcal{A}} \int_{\Omega} f^{(2)}(\mathbf{x}, \mathbf{w}) p(\mathbf{w}) d\mathbf{w}.$$

Figure 1 shows an example of the problem setup.

To identify a DR-PF, it is necessary to predict it and quantify its uncertainty. In this study, under the assumption that  $f^{(1)}(\mathbf{x}, \mathbf{w})$  and  $f^{(2)}(\mathbf{x}, \mathbf{w})$  follow a Gaussian process (GP), we developed a Bayesian optimization (BO) method to find a lower bound of the DR-PF by considering the uncertainty of environmental variables  $\mathbf{w}$  and the uncertainty of the probability distribution for  $\mathbf{w}$ . Specifically, we propose an acquisition function (AF) that enables us to sequentially select the controllable design variable  $\mathbf{x}$  in a sample-efficient manner to obtain the DR-PF.

To this end, various technical challenges need to be resolved. One difficulty is that, even when  $f^{(1)}(\mathbf{x}, \mathbf{w})$  and  $f^{(2)}(\mathbf{x}, \mathbf{w})$  are GPs,  $F^{(1)}(\mathbf{x})$  and  $F^{(2)}(\mathbf{x})$  are not GPs anymore. Therefore, we derive a non-trivial credible intervals of  $F^{(1)}(\mathbf{x})$  and  $F^{(2)}(\mathbf{x})$  considering that they are defined as the infima of integrated GPs. Furthermore, although a naive formulation of multi-objective BOs is computationally expensive, the proposed AF has the advantage that it can be evaluated efficiently. We also conducted a theoretical analysis of the proposed BO method to prove that the proposed BO method can find an arbitrarily accurate DR-PF with a high probability in a finite number of iterations under mild conditions.

### 1.1. Related Work

For black-box function optimization problems, BOs have been popularly used [Settles, 2009, Shahriari et al., 2016] in which GP [Williams and Rasmussen, 2006] is often employed as a surrogate model. An optimization problem

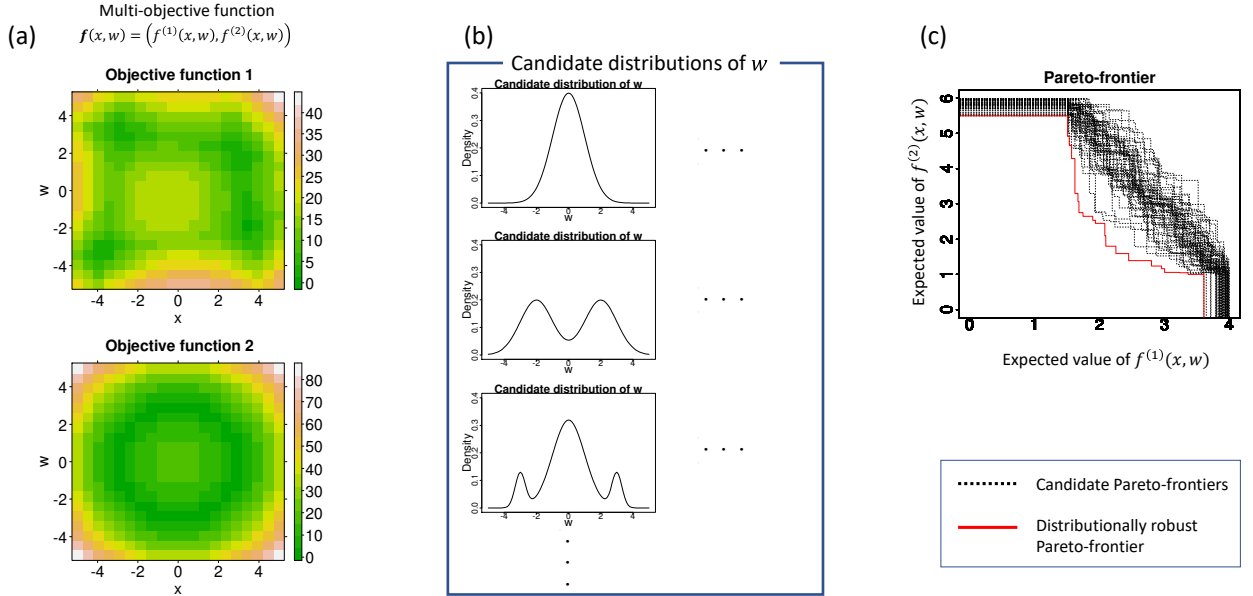


Figure 1: Conceptual diagram of a DR-PF. The upper and lower color maps in (a) represent objective functions  $f^{(1)}(x, w)$  and  $f^{(2)}(x, w)$ , respectively, where  $x$  and  $w$  are the scalar design and environmental variable, respectively. The plots within the frame in (b) represent multiple candidate distributions for  $w$ . A dashed line in (c) is the expected PF for each candidate distributions of  $w$ . A red solid line is the DR-PF, which is defined by the worst-case expectation of the candidate distributions, provides a lower bound of uncertain PF. The objective of this study is to efficiently identify the DR-PF.

of multiple black-box functions is typically formulated as a Pareto optimization problem, and BO methods for such problems have been also studied [Zuluaga et al., 2016, Suzuki et al., 2020].

Many studies have been conducted on BOs under uncertain environments. For example, [Bogunovic et al., 2018] proposed a BO method to maximize the worst-case function value with respect to a shift in the input. In several studies [Beland and Nair, 2017, Toscano-Palmerin and Frazier, 2018, Oliveira et al., 2019, Fröhlich et al., 2020, Gessner et al., 2020], a BO problem to maximize the expected value of a black-box function with respect to the input distribution was considered. Furthermore, several studies considered the simultaneous optimization of multiple black-box functions under the assumption that the distribution of environmental variables is known. For example, [Iwazaki et al., 2021] dealt with constrained optimization and Pareto optimization problems for the mean and variance of a black-box function with respect to environmental variables, [Qing et al., 2022] considered Pareto optimization problems for the expected values of multiple objective functions, and [Amri et al., 2021] dealt with chance-constrained optimization problems that is an extension of constrained optimization problems to the input uncertainty setting.

Distributionally robust optimization (DRO) was first introduced by [Scarf, 1958]. Because DRO is an important topic in the context of robust optimization and has been the subject of numerous studies, we refer an exhaustive survey of DRO to [Rahimian and Mehrotra, 2019]. In recent years, several studies on DRO in the context of BOs (DRO-BOs) have been conducted. [Kirschner et al., 2020] and [Nguyen et al., 2020] proposed BO methods to efficiently find the design variable that maximizes  $F^{(1)}(\mathbf{x})$ . DRO-BOs have also been studied under multiple black-box functions. [Inatsu et al., 2022] proposed a BO method for distributionally robust chance-constrained problems, which is an extension of the chance-constrained problem to DRO. However, to the best of our knowledge, there are no prior studies on BOs for Pareto optimization under the DRO framework.

## 1.2. Contributions

The contributions of this study are as follows:

- We develop a BO method for identifying DR-PFs called *DR-PF BO* method. Specifically, we propose a novel AF for the DR-PF BO, which is computationally inexpensive and has theoretical guarantees.
- Under mild conditions, we prove that the DR-PF BO method can find an arbitrarily accurate PF with a high probability in a finite number of iterations.
- Additionally, we prove that with a specification of an appropriate family of candidate distributions, even if the true distribution is unknown, the DR-PF BO method can find an arbitrarily accurate expected PF on the true distribution.

- We confirm the performance of the proposed method through numerical experiments with benchmark functions and simulator-based functions.

## 2. Preliminaries

Let  $f^{(1)} : \mathcal{X} \times \Omega \rightarrow \mathbb{R}$  and  $f^{(2)} : \mathcal{X} \times \Omega \rightarrow \mathbb{R}$  be the expensive-to-evaluate black-box functions<sup>1</sup>, where  $\mathcal{X}$  and  $\Omega$  are the finite sets. For each input  $(\mathbf{x}, \mathbf{w}) \in \mathcal{X} \times \Omega$ , the values of  $f^{(1)}(\mathbf{x}, \mathbf{w})$  and  $f^{(2)}(\mathbf{x}, \mathbf{w})$  are observed with observation noise as  $y^{(1)} = f^{(1)}(\mathbf{x}, \mathbf{w}) + \varepsilon^{(1)}$  and  $y^{(2)} = f^{(2)}(\mathbf{x}, \mathbf{w}) + \varepsilon^{(2)}$ , where  $\varepsilon^{(1)}$  and  $\varepsilon^{(2)}$  are random samples from independent normal distributions with the mean zero and variances  $\sigma_{\text{noise}}^{(1)2}$  and  $\sigma_{\text{noise}}^{(2)2}$ , respectively. In this study, the environmental variable  $\mathbf{w} \in \Omega$  was assumed to be a discrete random variable that follows an unknown probability distribution  $P^\dagger$ . The two distinct phases called the *development phase* and *use phase* exist in the literature of BOs under uncertainty. In the development phase, environmental variables are completely controllable as design variables, whereas they are stochastic and uncontrollable in the use phase. In this study, we consider the development phase, and the use phase is described in Appendix A. Furthermore, we denote the family of candidate distributions of  $\mathbf{w}$  as  $\mathcal{A}$  and consider the following class of distributions:

$$\mathcal{A} = \{p(\mathbf{w}) \mid d(p(\mathbf{w}), p^*(\mathbf{w})) \leq \xi\},$$

where  $p^*(\mathbf{w})$  is a user-specified reference distribution,  $d(\cdot, \cdot)$  is a given distance metric function between distributions, and  $\xi \geq 0$ . This means that we consider a set of candidate distributions whose distance from the reference distribution is not larger than a certain threshold. Subsequently, the distributionally robust expectations  $F^{(1)}(\mathbf{x})$  and  $F^{(2)}(\mathbf{x})$  for each design variable  $\mathbf{x} \in \mathcal{X}$  are defined as follows:

$$F^{(1)}(\mathbf{x}) = \inf_{p(\mathbf{w}) \in \mathcal{A}} \sum_{\mathbf{w} \in \Omega} f^{(1)}(\mathbf{x}, \mathbf{w}) p(\mathbf{w}),$$

$$F^{(2)}(\mathbf{x}) = \inf_{p(\mathbf{w}) \in \mathcal{A}} \sum_{\mathbf{w} \in \Omega} f^{(2)}(\mathbf{x}, \mathbf{w}) p(\mathbf{w}).$$

The objective of this study is to efficiently identify the PF determined by  $F^{(1)}(\mathbf{x})$  and  $F^{(2)}(\mathbf{x})$ . Let  $\mathbf{F}(\mathbf{x}) = (F^{(1)}(\mathbf{x}), F^{(2)}(\mathbf{x}))$  for each  $\mathbf{x} \in \mathcal{X}$ , and let  $\mathbf{F}(E) = \{\mathbf{F}(\mathbf{x}) \mid \mathbf{x} \in E\}$  for a set  $E \subset \mathcal{X}$ . Furthermore, for a set  $B \subset \mathbb{R}^2$ , we denote the domain dominated by  $B$  and the PF of  $B$ , respectively, by

$$\text{Dom}(B) = \{\mathbf{y} \in \mathbb{R}^2 \mid \exists \mathbf{y}' \in B \text{ s.t. } \mathbf{y} \preceq \mathbf{y}'\},$$

$$\text{Par}(B) = \partial(\text{Dom}(B)).$$

Here, for a point  $\mathbf{a} = (a_1, \dots, a_m)$  and  $\mathbf{b} = (b_1, \dots, b_m)$ ,  $\mathbf{a} \preceq \mathbf{b}$  implies  $a_i \leq b_i$  for any  $i \in \{1, \dots, m\}$ . For a set  $C$ ,  $\partial(C)$  denotes the boundary of  $C$ . The PF determined by  $F^{(1)}(\mathbf{x})$  and  $F^{(2)}(\mathbf{x})$  can then be written as

$$Z^* = \text{Par}(\mathbf{F}(\mathcal{X})).$$

### 2.1. Gaussian Process

In this study, we use GP surrogate models for black-box functions  $f^{(1)}$  and  $f^{(2)}$ . First, we assume that  $f^{(1)}$  and  $f^{(2)}$  follow GP priors  $\mathcal{GP}(0, k^{(1)}((\mathbf{x}, \mathbf{w}), (\mathbf{x}', \mathbf{w}')))$  and  $\mathcal{GP}(0, k^{(2)}((\mathbf{x}, \mathbf{w}), (\mathbf{x}', \mathbf{w}')))$ , respectively, where  $k^{(1)}((\mathbf{x}, \mathbf{w}), (\mathbf{x}', \mathbf{w}'))$  and  $k^{(2)}((\mathbf{x}, \mathbf{w}), (\mathbf{x}', \mathbf{w}'))$  are the positive-definite kernels. For  $l \in \{1, 2\}$ , given a dataset  $\{(\mathbf{x}_i, \mathbf{w}_i, y_i^{(l)})\}_{i=1}^t$ , where  $t$  is the number of queried instances, the posterior distribution of  $f^{(l)}$  is a GP, and its posterior mean  $\mu_t^{(l)}(\mathbf{x}, \mathbf{w})$  and posterior variance  $\sigma_t^{(l)2}(\mathbf{x}, \mathbf{w})$  are given by

$$\mu_t^{(l)}(\mathbf{x}, \mathbf{w}) = \mathbf{k}_t^{(l)}(\mathbf{x}, \mathbf{w})^\top (\mathbf{K}_t^{(l)} + \sigma_{\text{noise}}^{(l)2} \mathbf{I}_t)^{-1} \mathbf{y}_t^{(l)},$$

$$\sigma_t^{(l)2}(\mathbf{x}, \mathbf{w}) = k^{(l)}((\mathbf{x}, \mathbf{w}), (\mathbf{x}, \mathbf{w})) - \mathbf{k}_t^{(l)}(\mathbf{x}, \mathbf{w})^\top (\mathbf{K}_t^{(l)} + \sigma_{\text{noise}}^{(l)2} \mathbf{I}_t)^{-1} \mathbf{k}_t^{(l)}(\mathbf{x}, \mathbf{w}),$$

where  $\mathbf{k}_t^{(l)}(\mathbf{x}, \mathbf{w})$  is the  $t$ -dimensional vector, whose  $j$ th element is  $k^{(l)}((\mathbf{x}, \mathbf{w}), (\mathbf{x}_j, \mathbf{w}_j))$ ,  $\mathbf{y}_t^{(l)} = (y_1^{(l)}, \dots, y_t^{(l)})^\top$ ,  $\mathbf{I}_t$  is the  $t \times t$  identity matrix,  $\mathbf{K}_t^{(l)}$  is the  $t \times t$  matrix whose  $(j, k)$  element is  $k^{(l)}((\mathbf{x}_j, \mathbf{w}_j), (\mathbf{x}_k, \mathbf{w}_k))$ , with a superscript  $\top$  indicating the transpose of vectors or matrices.

## 3. Proposed Method

Here, we propose a BO method to efficiently identify  $Z^*$ . Because the functions  $f^{(1)}(\mathbf{x}, \mathbf{w})$  and  $f^{(2)}(\mathbf{x}, \mathbf{w})$  are random variables following GPs,  $F^{(1)}(\mathbf{x})$  and  $F^{(2)}(\mathbf{x})$  are also random variables. Therefore, a reasonable approach is to construct credible intervals for  $F^{(1)}(\mathbf{x})$  and  $F^{(2)}(\mathbf{x})$ , and use them to estimate the PF. However,

<sup>1</sup>Note that the method proposed in this study can be straightforwardly extended to the case where there are more than three objective functions  $f^{(1)}, f^{(2)}, f^{(3)}, \dots$

unlike  $f^{(1)}(\mathbf{x}, \mathbf{w})$  and  $f^{(2)}(\mathbf{x}, \mathbf{w})$ ,  $F^{(1)}(\mathbf{x})$  and  $F^{(2)}(\mathbf{x})$  do not follow GPs. Therefore, we cannot directly obtain credible intervals using the properties of GPs. In Section 3.1, we construct credible intervals for  $F^{(1)}(\mathbf{x})$  and  $F^{(2)}(\mathbf{x})$  using the method proposed by [Kirschner et al., 2020] and provide a method for estimating the PF based on the constructed credible intervals.

### 3.1. Credible Intervals and PF Estimation

For each input  $(\mathbf{x}, \mathbf{w}) \in \mathcal{X} \times \Omega$  and time  $t$ , the credible interval of  $f^{(1)}(\mathbf{x}, \mathbf{w})$  is denoted by  $Q_t^{(f^{(1)})}(\mathbf{x}, \mathbf{w}) = [l_t^{(f^{(1)})}(\mathbf{x}, \mathbf{w}), u_t^{(f^{(1)})}(\mathbf{x}, \mathbf{w})]$ . Here, the lower value  $l_t^{(f^{(1)})}(\mathbf{x}, \mathbf{w})$  and the upper value  $u_t^{(f^{(1)})}(\mathbf{x}, \mathbf{w})$  are given as

$$\begin{aligned} l_t^{(f^{(1)})}(\mathbf{x}, \mathbf{w}) &= \mu_t^{(1)}(\mathbf{x}, \mathbf{w}) - \beta_{1,t}^{1/2} \sigma_t^{(1)}(\mathbf{x}, \mathbf{w}), \\ u_t^{(f^{(1)})}(\mathbf{x}, \mathbf{w}) &= \mu_t^{(1)}(\mathbf{x}, \mathbf{w}) + \beta_{1,t}^{1/2} \sigma_t^{(1)}(\mathbf{x}, \mathbf{w}), \end{aligned}$$

where  $\beta_{1,t}^{1/2} \geq 0$  is a user-specified tradeoff parameter. We then define the credible interval  $Q_t^{(F^{(1)})}(\mathbf{x}) \equiv [l_t^{(F^{(1)})}(\mathbf{x}), u_t^{(F^{(1)})}(\mathbf{x})]$  of  $F^{(1)}(\mathbf{x})$ . Here, the lower and upper values are respectively given by

$$\begin{aligned} l_t^{(F^{(1)})}(\mathbf{x}) &= \inf_{p(\mathbf{w}) \in \mathcal{A}} \sum_{\mathbf{w} \in \Omega} l_t^{(f^{(1)})}(\mathbf{x}, \mathbf{w}) p(\mathbf{w}), \\ u_t^{(F^{(1)})}(\mathbf{x}) &= \inf_{p(\mathbf{w}) \in \mathcal{A}} \sum_{\mathbf{w} \in \Omega} u_t^{(f^{(1)})}(\mathbf{x}, \mathbf{w}) p(\mathbf{w}). \end{aligned} \tag{3.1}$$

Notably, if the  $L1$ - (or  $L2$ -) norm is used as the distance  $d(\cdot, \cdot)$  between the distributions, the problem of obtaining the lower and upper values in (3.1) is reduced to a linear programming problem (or a second-order cone programming problem). In either case, the existence of a fast solver of these problems enabled us to obtain  $Q_t^{(F^{(1)})}(\mathbf{x})$ . Similarly, we define credible intervals  $Q_t^{(f^{(2)})}(\mathbf{x}, \mathbf{w}) = [l_t^{(f^{(2)})}(\mathbf{x}, \mathbf{w}), u_t^{(f^{(2)})}(\mathbf{x}, \mathbf{w})]$  for  $f^{(2)}(\mathbf{x}, \mathbf{w})$  and  $Q_t^{(F^{(2)})}(\mathbf{x}) \equiv [l_t^{(F^{(2)})}(\mathbf{x}), u_t^{(F^{(2)})}(\mathbf{x})]$  for  $F^{(2)}(\mathbf{x})$ . Next, for any input  $\mathbf{x} \in \mathcal{X}$  and any subset  $E \subset \mathcal{X}$ , we define  $\mathbf{LCB}_t(\mathbf{x})$ ,  $\mathbf{UCB}_t(\mathbf{x})$  and  $\mathbf{LCB}_t(E)$  as follows:

$$\begin{aligned} \mathbf{LCB}_t(\mathbf{x}) &= (l_t^{(F^{(1)})}(\mathbf{x}), l_t^{(F^{(2)})}(\mathbf{x})), \\ \mathbf{UCB}_t(\mathbf{x}) &= (u_t^{(F^{(1)})}(\mathbf{x}), u_t^{(F^{(2)})}(\mathbf{x})), \\ \mathbf{LCB}_t(E) &= \{\mathbf{LCB}_t(\mathbf{x}) \mid \mathbf{x} \in E\}. \end{aligned}$$

The estimated PF solution set  $\hat{\Pi}_t \subset \mathcal{X}$  for the design variables is then defined as follows:

$$\hat{\Pi}_t = \{\mathbf{x} \in \mathcal{X} \mid \mathbf{LCB}_t(\mathbf{x}) \in \text{Par}(\mathbf{LCB}_t(\mathcal{X}))\}.$$

Figure 2 (a) shows a conceptual diagram of  $\mathbf{LCB}_t(\mathbf{x})$  and  $\mathbf{UCB}_t(\mathbf{x})$ , and (b) shows a conceptual diagram of  $\text{Par}(\mathbf{LCB}_t(\mathcal{X}))$  and  $\hat{\Pi}_t$ .

### 3.2. Acquisition Function

Here, we propose an AF for determining the next evaluation point. First, for each point  $\mathbf{a} \in \mathbb{R}^m$  and subset  $B \subset \mathbb{R}^m$ , we denote the closeness between them as

$$\text{dist}(\mathbf{a}, B) = \inf_{\mathbf{b} \in B} d_\infty(\mathbf{a}, \mathbf{b}),$$

where  $d_\infty(\mathbf{a}, \mathbf{b})$  denotes the metric function given by  $d_\infty(\mathbf{a}, \mathbf{b}) = \max\{|a_1 - b_1|, \dots, |a_m - b_m|\}$ . Using this, we define AF  $a_t(\mathbf{x})$  for  $\mathbf{x} \in \mathcal{X}$  as

$$a_t(\mathbf{x}) = \text{dist}(\mathbf{UCB}_t(\mathbf{x}), \text{Dom}(\mathbf{LCB}_t(\hat{\Pi}_t))).$$

We then select the following evaluation points, as described in the following definition:

**Definition 3.1.** The next design variable,  $\mathbf{x}_{t+1}$ , to be evaluated is selected as follows:

$$\mathbf{x}_{t+1} = \underset{\mathbf{x} \in \mathcal{X}}{\text{argmax}} a_t(\mathbf{x}),$$

and the next environmental variable,  $\mathbf{w}_{t+1}$ , to be evaluated is selected as

$$\mathbf{w}_{t+1} = \underset{\mathbf{w} \in \Omega}{\text{argmax}} \{\sigma_t^{(1)2}(\mathbf{x}_{t+1}, \mathbf{w}) + \sigma_t^{(2)2}(\mathbf{x}_{t+1}, \mathbf{w})\}.$$

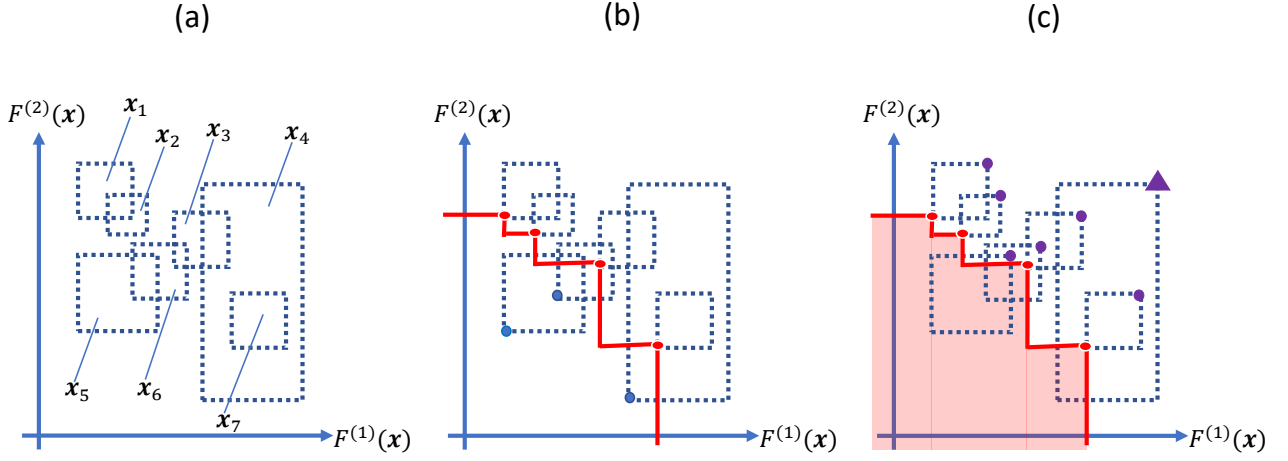


Figure 2: Conceptual diagrams of  $\mathbf{LCB}_t(\mathbf{x})$ ,  $\mathbf{UCB}_t(\mathbf{x})$ ,  $\text{Par}(\mathbf{LCB}_t(\mathcal{X}))$ ,  $\hat{\Pi}_t$  and AFs for seven input points  $\mathbf{x}_1, \dots, \mathbf{x}_7$ . At each point  $\mathbf{x}$  in the left figure (a),  $\mathbf{LCB}_t(\mathbf{x})$  and  $\mathbf{UCB}_t(\mathbf{x})$  indicate the lower left point and the upper right point of the dashed rectangular region, respectively. In (b), the PF (red line) computed using each  $\mathbf{LCB}_t(\mathbf{x})$  is  $\text{Par}(\mathbf{LCB}_t(\mathcal{X}))$ , and because it is constructed by  $\mathbf{LCB}_t(\mathbf{x}_1), \mathbf{LCB}_t(\mathbf{x}_2), \mathbf{LCB}_t(\mathbf{x}_3), \mathbf{LCB}_t(\mathbf{x}_7)$ ,  $\hat{\Pi}_t$  is given by  $\hat{\Pi}_t = \{\mathbf{x}_1, \mathbf{x}_2, \mathbf{x}_3, \mathbf{x}_7\}$ . In (c), the light red region indicates  $\text{Dom}(\mathbf{LCB}_t(\hat{\Pi}_t))$ , the region dominated by the red points ( $\mathbf{LCB}_t(\hat{\Pi}_t)$ ), and  $a_t(\mathbf{x})$  is the closeness between the light red region and  $\mathbf{UCB}_t(\mathbf{x})$  (purple point). The furthest point is represented by the purple triangle,  $\mathbf{UCB}_t(\mathbf{x}_4)$ . Thus, the next design variable to be evaluated is  $\mathbf{x}_4$ .

Figure 2 (c) shows a conceptual diagram of the AF  $a_t(\mathbf{x})$ . Here, AF  $a_t(\mathbf{x})$  can be computed analytically using the following lemma:

**Lemma 3.1.** Let  $\mathbf{UCB}_t(\mathbf{x}) = (u_1, u_2)$  and  $\mathbf{LCB}_t(\hat{\Pi}_t) = \{(l_1^{(i)}, l_2^{(i)}) \mid 1 \leq i \leq k\}$ . Then,  $a_t(\mathbf{x})$  can be computed as follows:

$$\begin{aligned} \tilde{a}_t(\mathbf{x}) &= \min_{1 \leq i \leq k} \max\{u_1 - l_1^{(i)}, u_2 - l_2^{(i)}\}, \\ a_t(\mathbf{x}) &= \max\{\tilde{a}_t(\mathbf{x}), 0\}. \end{aligned}$$

Notably, when the number of objective functions is  $m \geq 3$ ,  $a_t(\mathbf{x})$  is easily extended as follows:

$$\begin{aligned} \tilde{a}_t(\mathbf{x}) &= \min_{1 \leq i \leq k'} \max\{u_1 - l_1^{(i)}, \dots, u_m - l_m^{(i)}\}, \\ a_t(\mathbf{x}) &= \max\{\tilde{a}_t(\mathbf{x}), 0\}, \end{aligned} \tag{3.2}$$

where  $\mathbf{UCB}_t(\mathbf{x}) = (u_1, \dots, u_m)$  and  $\mathbf{LCB}_t(\hat{\Pi}_t) = \{(l_1^{(i)}, \dots, l_m^{(i)}) \mid 1 \leq i \leq k'\}$ . The proofs of Lemma 3.1 and (3.2) are presented in Appendix B. From Lemma 3.1, once  $\mathbf{LCB}_t(\hat{\Pi}_t)$  is computed, the maximum value of  $a_t(\mathbf{x})$  can be analytically obtained by performing  $2|\mathcal{X}|$  times inf calculations and computing  $u_t^{(F^{(1)})}(\mathbf{x})$  and  $u_t^{(F^{(2)})}(\mathbf{x})$  for all  $\mathbf{x} \in \mathcal{X}$ . On the other hand, an AF based on exact posterior distributions of target functions such as the expected hypervolume improvement [Emmerich, 2005] for ordinary Pareto optimization, requires approximation by sampling from  $f^{(1)}(\mathbf{x}, \mathbf{w})$  and  $f^{(2)}(\mathbf{x}, \mathbf{w})$  under this problem setting. However, in each posterior sample, the inf calculation must be performed again to calculate  $F^{(1)}(\mathbf{x})$  and  $F^{(2)}(\mathbf{x})$  for all design variables. Therefore, if the number of Monte Carlo samples is  $M$ ,  $M$  times more inf calculations are required compared to the proposed AF. The comparison of computational times is given in Section 5.

### 3.3. Stopping Condition

Here, we describe the stopping conditions of the proposed algorithm. From Fig. 2 (c), AF  $a_t(\mathbf{x})$  represents the closeness of the pessimistic PF and the optimistic predictive value of  $\mathbf{F}(\mathbf{x})$ . That is, if this value is sufficiently small, there is little room for improvement in the PF; therefore, it is reasonable to use it as the stopping condition. Let  $\epsilon > 0$  be a user-specified parameter. Then the algorithm is terminated if  $a_t(\mathbf{x}) \leq \epsilon$  is satisfied. The pseudocode for the proposed algorithm is given in Algorithm 1.

## 4. Theoretical Analysis

Here, we provide the theorems for the accuracy and convergence of the proposed algorithm. The details of the proofs are presented in Appendix B. First, to provide theoretical results, we assume that  $f^{(1)}$  and  $f^{(2)}$  follow

---

**Algorithm 1** BO for identifying DR-PF

---

**Input:** GP priors  $\mathcal{GP}(0, k^{(1)})$ ,  $\mathcal{GP}(0, k^{(2)})$ , parameter  $\xi \geq 0$ , tradeoff parameters  $\{\beta_{1,t}\}_{t \geq 0}$ ,  $\{\beta_{2,t}\}_{t \geq 0}$ , stopping parameter  $\epsilon > 0$

$t \leftarrow 1$

**while**  $a_t(\mathbf{x}) > \epsilon$  **do**

    Compute  $Q_t^{(F^{(1)})}(\mathbf{x})$  and  $Q_t^{(F^{(2)})}(\mathbf{x})$  for each  $\mathbf{x} \in \mathcal{X}$

    Select the next evaluation point  $(\mathbf{x}_t, \mathbf{w}_t)$

    Observe  $y_t^{(1)} = f^{(1)}(\mathbf{x}_t, \mathbf{w}_t) + \varepsilon_t^{(1)}$  and  $y_t^{(2)} = f^{(2)}(\mathbf{x}_t, \mathbf{w}_t) + \varepsilon_t^{(2)}$  at the point  $(\mathbf{x}_t, \mathbf{w}_t)$

    Update GPs by adding observed points

$t \leftarrow t + 1$

**end while**

**Output:** Return  $\hat{\Pi}_t$  as the estimated set of design variables comprising the DR-PF

---

GPs  $\mathcal{GP}(0, k^{(1)}((\mathbf{x}, \mathbf{w}), (\mathbf{x}', \mathbf{w}')))$  and  $\mathcal{GP}(0, k^{(2)}((\mathbf{x}, \mathbf{w}), (\mathbf{x}', \mathbf{w}')))$ , respectively. Moreover, we assume that the prior variances  $k^{(1)}((\mathbf{x}, \mathbf{w}), (\mathbf{x}, \mathbf{w})) \equiv \sigma_0^{(1)2}(\mathbf{x}, \mathbf{w})$  and  $k^{(2)}((\mathbf{x}, \mathbf{w}), (\mathbf{x}, \mathbf{w})) \equiv \sigma_0^{(2)2}(\mathbf{x}, \mathbf{w})$  satisfy

$$\begin{aligned} \max_{(\mathbf{x}, \mathbf{w}) \in \mathcal{X} \times \Omega} \sigma_0^{(1)2}(\mathbf{x}, \mathbf{w}) &\leq 1, \\ \max_{(\mathbf{x}, \mathbf{w}) \in \mathcal{X} \times \Omega} \sigma_0^{(2)2}(\mathbf{x}, \mathbf{w}) &\leq 1. \end{aligned}$$

Furthermore, let  $\kappa_T^{(1)}$  and  $\kappa_T^{(2)}$  be the maximum information gains of  $f^{(1)}$  and  $f^{(2)}$  at time  $T$ , respectively. Notably, the maximum information gain is a measure often used in theoretical analyses of GP-based BO (see, e.g., [Srinivas et al., 2010]). Here, for each  $j \in \{1, 2\}$ , using the mutual information  $I(\mathbf{y}^{(j)}; f^{(j)})$  between  $\mathbf{y}^{(j)}$  and  $f^{(j)}$ ,  $\kappa_T^{(j)}$  can be expressed as

$$\kappa_T^{(j)} = \max_{A \subset \mathcal{X} \times \Omega} I(\mathbf{y}_A^{(j)}; f^{(j)}).$$

Next, to quantify the goodness of the predicted  $\hat{\Pi}_t$ , we define an  $\epsilon$ -accurate Pareto region  $Z_\epsilon$ . With user-specified positive numbers  $\epsilon$  and  $\epsilon = (\epsilon, \epsilon)$ , we define  $Z_\epsilon$  as

$$Z_\epsilon = \{\mathbf{y} \in \mathbb{R}^2 \mid \exists \mathbf{y}' \in Z^* \text{ s.t. } \mathbf{y} \preceq \mathbf{y}' \text{ and } \exists \mathbf{y}'' \in Z^* \text{ s.t. } \mathbf{y}'' \preceq \mathbf{y} + \epsilon\}.$$

That is,  $Z_\epsilon$  is the set of points that lie inside  $Z^*$  and within  $\epsilon$  in the sense of  $d_\infty(\cdot, \cdot)$ -distance. The concept of  $Z_\epsilon$  was also used in [Zuluaga et al., 2016]. Using  $Z_\epsilon$ , we define the accuracy of  $\hat{\Pi}_t$  in terms of the following two aspects:

**Definition 4.1** (Accuracy for  $\hat{\Pi}_t$ ). Let  $\epsilon$  be a positive value. We then define  $\hat{\Pi}_t$  as an  $\epsilon$ -accurate estimated solution set if the following holds:

$$\mathbf{F}(\hat{\Pi}_t) \subset Z_\epsilon. \quad (4.1)$$

Moreover, we define  $\hat{\Pi}_t$  as an  $\epsilon$ -accurate estimated Pareto solution set if the following holds:

$$\text{Par}(\mathbf{F}(\hat{\Pi}_t)) \subset Z_\epsilon. \quad (4.2)$$

It is easy to obtain a set that satisfies either (4.1) or (4.2). Generally, by ignoring  $F^{(2)}(\mathbf{x})$  and focusing only on the maximization of  $F^{(1)}(\mathbf{x})$ , the maximization point  $\mathbf{x}^*$  can be estimated using methods such as [Kirschner et al., 2020]. Subsequently, by letting  $\hat{\Pi}_t = \{\mathbf{x}^*\}$ , (4.1) is satisfied with high probability. Similarly, if we predict that all points constitute the PF, that is,  $\hat{\Pi}_t = \mathcal{X}$ , then (4.2) is satisfied because  $\text{Par}(\mathbf{F}(\hat{\Pi}_t)) = \text{Par}(\mathbf{F}(\mathcal{X})) = Z^*$ . The following theorem guarantees that the proposed algorithm satisfies both (4.1) and (4.2) with a high probability.

**Theorem 4.1.** Let  $t \geq 1$  and  $\delta \in (0, 1)$  and define  $\beta_{1,t} = \beta_{2,t} = 2 \log(2|\mathcal{X} \times \Omega| \pi^2 t^2 / (6\delta)) \equiv \beta_t$ . In addition, let  $\epsilon > 0$  be a user-specified stopping parameter. Then, when Algorithm 1 terminates,  $\hat{\Pi}_t$  satisfies (4.1) and (4.2) with a probability of at least  $1 - \delta$ .

Theorem 4.1 does not indicate whether the algorithm terminates or not. The following theorem guarantees the convergence of Algorithm 1.

**Theorem 4.2.** Under the same conditions as those in Theorem 4.1, let  $T$  be the smallest positive integer that satisfies the following inequality:

$$\frac{\beta_T(C_1 \kappa_T^{(1)} + C_2 \kappa_T^{(2)})}{T} \leq \frac{\epsilon^2}{4},$$

where  $C_1 = 2/\log(1 + \sigma_{\text{noise}}^{(1)-2})$  and  $C_2 = 2/\log(1 + \sigma_{\text{noise}}^{(2)-2})$ . Then, Algorithm 1 terminates after at most  $T$  trials.

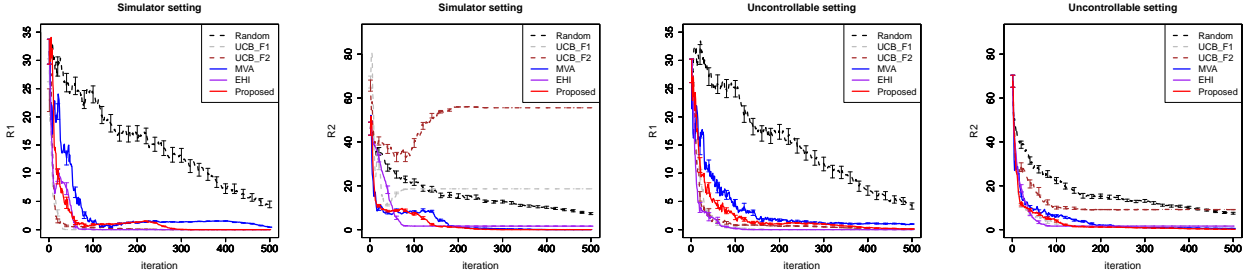


Figure 3: Average values of  $R1$  and  $R2$  for each method in Simulator and Uncontrollable settings. The length of each error bar represents twice the standard error.

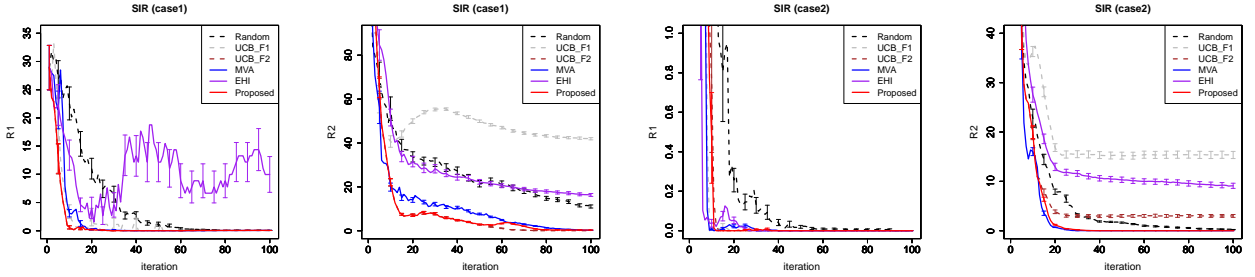


Figure 4: Average values of  $R1$  and  $R2$  for each method in Case1 and Case2 in SIR model experiments. The length of each error bar represents twice the standard error.

Table 1: Computational time (second) and the ratios of the computational time to that of the proposed method

	Random	UCB_F1	UCB_F2	MVA	EHI	Proposed
Computational time	0.000	0.068	0.067	0.135	16.21	0.139
(Standard error)	(0.000)	(0.000)	(0.000)	(0.001)	(0.011)	(0.001)
Computational time ratio	0.000	0.496	0.488	0.985	118.68	1
(Standard error)	(0.000)	(0.004)	(0.004)	(0.006)	(0.548)	(0)

Here, because the maximum information gains  $\kappa_T^{(1)}$  and  $\kappa_T^{(2)}$  are known to be sublinear with respect to  $T$  under mild assumptions [Srinivas et al., 2010], and the order of  $\beta_{1,T} = \beta_{2,T}$  is  $O(\log T)$ , the positive integer  $T$  satisfying the inequality in Theorem 4.2 exists.

We emphasize that Theorem 4.1 also holds in the use phase setting and a similar theorem holds for Theorem 4.2 under mild additional conditions. Moreover, by appropriately designing the family of candidate distributions using the empirical distribution as the reference distribution, the proposed method provides an arbitrarily accurate solution for the expected PF based on the true distribution, even when the true distribution is unknown. Details are provided in Appendix A.

## 5. Numerical Experiments

Here, we confirm the performance of the proposed method using synthetic functions and real-world simulation models. In this experiment, we used a one-dimensional design variable  $x$  and environmental variable  $w$  and the following Gaussian kernels:

$$k^{(1)}((x, w), (x', w')) = \sigma_{f,1}^2 \exp(-\|\boldsymbol{\nu} - \boldsymbol{\nu}'\|_2^2 / L_1),$$

$$k^{(2)}((x, w), (x', w')) = \sigma_{f,2}^2 \exp(-\|\boldsymbol{\nu} - \boldsymbol{\nu}'\|_2^2 / L_2),$$

where  $\boldsymbol{\nu} = (x, w)$  and  $\boldsymbol{\nu}' = (x', w')$ . Moreover, we used the  $L1$ -norm as the distance between distributions. In all experiments except computational time experiments, we used the following two indicators  $R1$  and  $R2$  based on (4.1) and (4.2) to evaluate the goodness of  $\hat{\Pi}_t$  estimated by each method:

$$R1 = \inf\{a \in \mathbb{R} \mid \mathbf{F}(\hat{\Pi}_t) \subset Z_a\},$$

$$R2 = \inf\{a \in \mathbb{R} \mid \text{Par}(\mathbf{F}(\hat{\Pi}_t)) \subset Z_a\}.$$

Experimental details and additional experiments, which are not included in the main body, are described in Appendix C.

## 5.1. Synthetic Function

We evaluate the performance in our proposed method through synthetic functions. First, the input space  $\mathcal{X} \times \Omega$  was a set of  $50 \times 50$  grid points equally spaced in  $[-10, 10] \times [-10, 10]$ . In this experiment, we used the following (scaled) Himmelblau’s function  $f^{(1)}(x, w)$ , which is commonly used as a benchmark function in BO studies [Andrei, 2008], and sinusoidal function  $f^{(2)}(x, w)$  as black-box functions:

$$f^{(1)}(x, w) = \frac{(x^2 + w - 11)^2}{150} + \frac{(x + w^2 - 7)^2}{150} - C,$$

$$f^{(2)}(x, w) = (80 \sin(1.5x) - 50 \cos(2w))/1.5,$$

where  $C = 3321.291/150$  is a constant to set the mean to zero.

Under this setting, we compared the following six methods:

**Random:** Determine the next evaluation point  $x_{t+1}$  at random.

**UCB\_F1:** Select the next evaluation point by  $x_{t+1} = \operatorname{argmax}_{x \in \mathcal{X}} u_t^{(F^{(1)})}(x)$ .

**UCB\_F2:** Select the next evaluation point by  $x_{t+1} = \operatorname{argmax}_{x \in \mathcal{X}} u_t^{(F^{(2)})}(x)$ .

**MVA:** Select the next evaluation point by  $x_{t+1} = \operatorname{argmax}_{x \in M_t \cup \hat{\Pi}_t} \lambda_t(x)$ , where  $M_t$  and  $\lambda_t(x)$  are given in Section 3.2 of [Iwazaki et al., 2021].

**EHI:** Select the next evaluation point  $x_{t+1}$  by maximizing an expected hypervolume improvement for the DR-PF calculated based on posterior means.

**Proposed:** Select the next evaluation point  $x_{t+1}$  by Definition 3.1.

Here, **UCB\_F1** (or **UCB\_F2**) focuses on the maximization of  $F^{(1)}(x)$  (or  $F^{(2)}(x)$ ) and does not consider the identification of the DR-PF. In contrast, **MVA** focuses on reducing the uncertainty of a potential optimal set, which is a set of input points that may constitute the DR-PF. The **EHI** method is the strategy that extends the expected hypervolume improvement strategy, which is commonly used in BO for ordinary Pareto optimization problems, to the DR-PF identification problem. Because the expected hypervolume improvement for the DR-PF cannot be calculated analytically, we approximated it using Monte Carlo sampling with a sample size of 100. Experiments were conducted under the following two settings for the observation of  $w$ :

**Simulator setting:** At each time  $t$ , arbitrary  $w$  can be selected.

**Uncontrollable setting:** At each time  $t$ ,  $w$  cannot be selected and is observed as a random sample from the uniform distribution on  $\Omega$ .

The **Simulator setting** and **Uncontrollable setting** correspond to the development phase and use phase, respectively. In **Simulator setting**, we used  $p^*(w) = 1/50$ , and the next environmental variable to be evaluate for each method except **Random** was selected by

$$w_{t+1} = \operatorname{argmax}_{w \in \Omega} (\sigma_t^{(1)2}(x_{t+1}, w) + \sigma_t^{(2)2}(x_{t+1}, w)).$$

In **Random**,  $w_{t+1}$  was selected as a random sample from the uniform distribution on  $\Omega$ . In **Uncontrollable setting**, we allowed the use of a different reference distribution  $p_t^*(w)$  for each iteration  $t$  and used the empirical distribution of  $w$  as  $p_t^*(w)$ .

Under this setup, one initial point was taken at random and the algorithm was run until the number of iterations reached 500. This simulation was repeated 100 times and the average values of  $R1$  and  $R2$  at each iteration were calculated. From Fig. 3, it can be confirmed that  $R1$  and  $R2$  in **Random** are not zero even after 500 iterations for both settings. In **UCB\_F1** and **UCB\_F2**, the value of  $R1$  is good but the value of  $R2$  is not good because they focus on one of the black-box functions. For **MVA**, **EHI**, and **Proposed**, which focus on improving the DR-PF,  $R1$  and  $R2$  tend to be zero in both settings, but **Proposed** converges to zero more quickly.

## 5.2. Computational Time Experiments

We confirmed the computational time required to select  $x_{t+1}$  and  $w_{t+1}$  using each method. We performed the same experiment as in **Simulator setting** in the previous section to evaluate the computational time. Under this setup, one initial point was taken at random and the algorithm was run until the number of iterations reached 500. We computed the average computational time over 500 iterations. We also computed the ratio of the computational time of each method to that of the proposed method. From Table 1, it can be confirmed that **Random**, which does not require inf calculations, is faster than the proposed method, and **UCB\_F1** (or



**UCB\_F2**), which uses only  $u_t^{(F^{(1)})}(x)$  (or  $u_t^{(F^{(2)})}(x)$ ) required inf calculations, is about half the computational time of the proposed method. The proposed method and **MVA** using both  $u_t^{(F^{(1)})}(x)$  and  $u_t^{(F^{(2)})}(x)$  have comparable computational speed. On the other hand, **EHI**, which performs the same number of inf calculations for each Monte Carlo sample as the proposed method requires, takes about 100 times longer than the proposed method because the number of Monte Carlo samples is 100.

### 5.3. Infection Simulation

We applied the proposed method to the Pareto optimization problem using a simulation model of a real-world infectious disease. We used the SIR model [Kermack and McKendrick, 1927], which is commonly used as the infection simulation model. In this experiment, we used the SIR model which has the infection rate  $\beta \in [0, 1]$  and the recovery  $\gamma \in [0, 1]$ . The input space  $\mathcal{X} \times \Omega$  was defined as the set of grid points when the region  $[0.01, 0.5] \times [0.01, 0.5]$  was equally divided into  $50 \times 50$  grid points. Using the SIR model, we defined the following two risk functions which can be interpreted as economic risks:

$$\begin{aligned} r_1(\beta, \gamma) &= n(\beta, \gamma) - 450\beta + 800\gamma - C_1, \\ r_2(\beta, \gamma) &= n(\beta, \gamma) - C_2, \end{aligned}$$

where  $n(\beta, \gamma)$  is the maximum number of infected individuals during a given period, calculated using the SIR model, and  $C_1$  and  $C_2$  are constants. Notably,  $r_1(\beta, \gamma)$  and  $r_2(\beta, \gamma)$  were also used in [Inatsu et al., 2022]. In this experiment, we used the same parameter setting as them. To adapt it to our problem setup, we multiplied them by minus one because risk functions should be minimized. Because  $\beta$  and  $\gamma$  can be interpreted as both design variables and environmental variables, we considered the following two cases:

**Case1:**  $f^{(1)}(x, w) = -r_1(x, w)$  and  $f^{(2)}(x, w) = -r_2(x, w)$ , where  $x$  and  $w$  are the infection rate and recovery rate, respectively.

**Case2:**  $f^{(1)}(x, w) = -r_1(x, w)$  and  $f^{(2)}(x, w) = -r_2(x, w)$ , where  $x$  and  $w$  are the recovery rate and infection rate, respectively.

In this experiment, we considered **Simulator setting** as in Section 5.1.

Under this setup, one initial point was taken at random and the algorithm was run until the number of iterations reached 100. This simulation was repeated 100 times and the average values of  $R1$  and  $R2$  at each iteration were calculated. From Fig. 4, it can be confirmed that the proposed method achieves equal or better performance in all settings.

## 6. Conclusion

In this study, we proposed an efficient BO method for identifying the DR-PF. We proved that the proposed method has theoretical guarantees on accuracy and convergence. Furthermore, through numerical experiments, we confirmed that the proposed method outperforms other comparative methods. Future work includes extending the method to the case where  $\mathbf{w}$  is a continuous random variable.

## Acknowledgement

This work was partially supported by MEXT KAKENHI (20H00601), JST CREST (JPMJCR21D3, JPMJCR21D3), JST Moonshot R&D (JPMJMS2033-05), JST AIP Acceleration Research (JPMJCR21U2), NEDO (JPNP18002, JPNP20006) and RIKEN Center for Advanced Intelligence Project.

## References

- [Amri et al., 2021] Amri, R. E., Riche, R. L., Helbert, C., Blanchet-Scalliet, C., and Da Veiga, S. (2021). A sampling criterion for constrained bayesian optimization with uncertainties. *arXiv preprint arXiv:2103.05706*.
- [Andrei, 2008] Andrei, N. (2008). An unconstrained optimization test functions collection. *Adv. Model. Optim.*, 10(1):147–161.
- [Beland and Nair, 2017] Beland, J. J. and Nair, P. B. (2017). Bayesian optimization under uncertainty. In *NIPS BayesOpt 2017 workshop*.
- [Bogunovic et al., 2018] Bogunovic, I., Scarlett, J., Jegelka, S., and Cevher, V. (2018). Adversarially robust optimization with Gaussian processes. In *Advances in neural information processing systems*, pages 5760–5770.
- [Emmerich, 2005] Emmerich, M. (2005). *Single-and multi-objective evolutionary design optimization assisted by gaussian random field metamodels*. PhD thesis, Dortmund, Univ., Diss., 2005.

- [Fröhlich et al., 2020] Fröhlich, L., Klenske, E., Vinogradska, J., Daniel, C., and Zeilinger, M. (2020). Noisy-input entropy search for efficient robust bayesian optimization. In Chiappa, S. and Calandra, R., editors, *Proceedings of the Twenty Third International Conference on Artificial Intelligence and Statistics*, volume 108 of *Proceedings of Machine Learning Research*, pages 2262–2272. PMLR.
- [Gessner et al., 2020] Gessner, A., Gonzalez, J., and Mahsereci, M. (2020). Active multi-information source Bayesian quadrature. In *Uncertainty in Artificial Intelligence*, pages 712–721. PMLR.
- [Inatsu et al., 2022] Inatsu, Y., Takeno, S., Karasuyama, M., and Takeuchi, I. (2022). Bayesian optimization for distributionally robust chance-constrained problem. In Chaudhuri, K., Jegelka, S., Song, L., Szepesvari, C., Niu, G., and Sabato, S., editors, *Proceedings of the 39th International Conference on Machine Learning*, volume 162 of *Proceedings of Machine Learning Research*, pages 9602–9621. PMLR.
- [Iwazaki et al., 2021] Iwazaki, S., Inatsu, Y., and Takeuchi, I. (2021). Mean-variance analysis in bayesian optimization under uncertainty. In Banerjee, A. and Fukumizu, K., editors, *Proceedings of The 24th International Conference on Artificial Intelligence and Statistics*, volume 130 of *Proceedings of Machine Learning Research*, pages 973–981. PMLR.
- [Kermack and McKendrick, 1927] Kermack, W. O. and McKendrick, A. G. (1927). A contribution to the mathematical theory of epidemics. *Proceedings of the royal society of london. Series A, Containing papers of a mathematical and physical character*, 115(772):700–721.
- [Kirschner et al., 2020] Kirschner, J., Bogunovic, I., Jegelka, S., and Krause, A. (2020). Distributionally robust Bayesian optimization. In Chiappa, S. and Calandra, R., editors, *Proceedings of the Twenty Third International Conference on Artificial Intelligence and Statistics*, volume 108 of *Proceedings of Machine Learning Research*, pages 2174–2184. PMLR.
- [Kirschner and Krause, 2018] Kirschner, J. and Krause, A. (2018). Information directed sampling and bandits with heteroscedastic noise. In *Conference On Learning Theory*, pages 358–384. PMLR.
- [Nguyen et al., 2020] Nguyen, T., Gupta, S., Ha, H., Rana, S., and Venkatesh, S. (2020). Distributionally robust Bayesian quadrature optimization. In Chiappa, S. and Calandra, R., editors, *Proceedings of the Twenty Third International Conference on Artificial Intelligence and Statistics*, volume 108 of *Proceedings of Machine Learning Research*, pages 1921–1931. PMLR.
- [Oliveira et al., 2019] Oliveira, R., Ott, L., and Ramos, F. (2019). Bayesian optimisation under uncertain inputs. In *The 22nd International Conference on Artificial Intelligence and Statistics*, pages 1177–1184.
- [Qing et al., 2022] Qing, J., Couckuyt, I., and Dhaene, T. (2022). A robust multi-objective bayesian optimization framework considering input uncertainty. *arXiv preprint arXiv:2202.12848*.
- [Rahimian and Mehrotra, 2019] Rahimian, H. and Mehrotra, S. (2019). Distributionally robust optimization: A review. *arXiv preprint arXiv:1908.05659*.
- [Scarf, 1958] Scarf, H. (1958). A min-max solution of an inventory problem. *Studies in the mathematical theory of inventory and production*, 10:201–209.
- [Settles, 2009] Settles, B. (2009). Active learning literature survey. Technical report, University of Wisconsin-Madison Department of Computer Sciences.
- [Shahriari et al., 2016] Shahriari, B., Swersky, K., Wang, Z., Adams, R. P., and De Freitas, N. (2016). Taking the human out of the loop: A review of Bayesian optimization. *Proceedings of the IEEE*, 104(1):148–175.
- [Srinivas et al., 2010] Srinivas, N., Krause, A., Kakade, S., and Seeger, M. (2010). Gaussian process optimization in the bandit setting: No regret and experimental design. In *Proceedings of the 27th International Conference on International Conference on Machine Learning, ICML’10*, pages 1015–1022, USA. Omnipress.
- [Suzuki et al., 2020] Suzuki, S., Takeno, S., Tamura, T., Shitara, K., and Karasuyama, M. (2020). Multi-objective bayesian optimization using pareto-frontier entropy. In *International Conference on Machine Learning*, pages 9279–9288. PMLR.
- [Toscano-Palmerin and Frazier, 2018] Toscano-Palmerin, S. and Frazier, P. I. (2018). Bayesian optimization with expensive integrands. *arXiv preprint arXiv:1803.08661*.
- [Williams and Rasmussen, 2006] Williams, C. K. and Rasmussen, C. E. (2006). Gaussian processes for machine learning. *the MIT Press*, 2(3):4.
- [Zuluaga et al., 2016] Zuluaga, M., Krause, A., and Püschel, M. (2016).  $\epsilon$ -pal: an active learning approach to the multi-objective optimization problem. *The Journal of Machine Learning Research*, 17(1):3619–3650.

## Appendix

### A. Generalization of Problem Setup

Here, we consider a more general problem setting, including the setting introduced in the main text. Specifically, we consider the following three settings:

- The case with three or more objective functions.
- Environment variables cannot be controlled even during optimization.
- The setting where reference distributions, control parameter  $\xi$ , and candidate distribution family  $\mathcal{A}$  set differently at each time.

Furthermore, by combining (ii) and (iii), we show that under appropriate assumptions, the solution to the distributionally robust Pareto optimization problem is also a good solution to the Pareto optimization problem defined by the true expectation.

#### A.1. Extended Problem Setting

Let  $f^{(1)}, \dots, f^{(m)} : \mathcal{X} \times \Omega \rightarrow \mathbb{R}$  be expensive-to-evaluate black-box functions, where  $2 \leq m$ . Also let  $\mathcal{X}$  and  $\Omega$  be finite sets. Here, for each  $(\mathbf{x}, \mathbf{w}) \in \mathcal{X} \times \Omega$  and  $j \in \{1, \dots, m\} \equiv [m]$ , the value of  $f^{(j)}(\mathbf{x}, \mathbf{w})$  is observed with Gaussian noise  $\varepsilon^{(j)}$  as  $y^{(j)} = f^{(j)}(\mathbf{x}, \mathbf{w}) + \varepsilon^{(j)}$ , where  $\varepsilon^{(1)}, \dots, \varepsilon^{(m)}$  are mutually independent, and  $\varepsilon^{(j)}$  follows Normal distribution with mean zero and variance  $\sigma_{\text{noise}}^{(j)2}$ , that is,  $\varepsilon^{(j)} \sim \mathcal{N}(0, \sigma_{\text{noise}}^{(j)2})$ . In this section, we assume that  $\mathbf{w} \in \Omega$  is a discrete random variable and follows some unknown distribution  $P^\dagger$ . Here, for environmental variables, we consider either settings in the development phase or settings in the use phase. That is, in the former, environmental variables are completely controllable as design variables; in the latter, environmental variables are uncontrollable and observed as realizations from the true distribution. Furthermore, let  $\mathcal{A}_t$  denote the candidate distribution family of  $P^\dagger$  at each time  $t$ , and consider the following  $\mathcal{A}_t$ :

$$\mathcal{A}_t = \{p(\mathbf{w}) \mid d(p(\mathbf{w}), p_t^*(\mathbf{w})) \leq \xi_t\},$$

where  $p_t^*(\mathbf{w})$  is a user-specified reference distribution,  $d(\cdot, \cdot)$  is a given distance function between distributions, and  $\xi_t \geq 0$ . Then, for each design variable  $\mathbf{x} \in \mathcal{X}$  and time  $t$ , the distributionally robust expectations  $F_t^{(1)}(\mathbf{x}), \dots, F_t^{(m)}(\mathbf{x})$  are defined as follows:

$$F_t^{(j)}(\mathbf{x}) = \inf_{p(\mathbf{w}) \in \mathcal{A}_t} \sum_{\mathbf{w} \in \Omega} f^{(j)}(\mathbf{x}, \mathbf{w}) p(\mathbf{w}), \quad j \in [m].$$

Hereafter, we aim to efficiently identify the PF  $Z_t^*$  determined by  $F_t^{(1)}(\mathbf{x}), \dots, F_t^{(m)}(\mathbf{x})$ . For each  $\mathbf{x} \in \mathcal{X}$ , subset  $E \subset \mathcal{X}$  and time  $t$ , let  $\mathbf{F}_t(\mathbf{x}) = (F_t^{(1)}(\mathbf{x}), \dots, F_t^{(m)}(\mathbf{x}))$  and  $\mathbf{F}_t(E) = \{\mathbf{F}_t(\mathbf{x}) \mid \mathbf{x} \in E\}$ . Moreover, for a set  $B \subset \mathbb{R}^m$ , the domain  $\text{Dom}(B)$  dominated by  $B$  and the Pareto-frontier  $\text{Par}(B)$  of  $B$  are given by

$$\begin{aligned} \text{Dom}(B) &= \{\mathbf{y} \in \mathbb{R}^m \mid \exists \mathbf{y}' \in B \text{ s.t. } \mathbf{y} \preceq \mathbf{y}'\}, \\ \text{Par}(B) &= \partial(\text{Dom}(B)). \end{aligned}$$

Then, the PF  $Z_t^*$  defined by  $F_t^{(1)}(\mathbf{x}), \dots, F_t^{(m)}(\mathbf{x})$  can be expressed as follows:

$$Z_t^* = \text{Par}(\mathbf{F}_t(\mathcal{X})).$$

##### A.1.1. Gaussian Process

Next, we construct predictive models for the black-box functions. As in the main body, GPs are used to model the black-box functions  $f^{(1)}, \dots, f^{(m)}$ . First, for each  $j \in [m]$ , assume that  $f^{(j)}$  follows a GP prior  $\mathcal{GP}(0, k^{(j)}((\mathbf{x}, \mathbf{w}), (\mathbf{x}', \mathbf{w}')))$ , where  $k^{(j)}((\mathbf{x}, \mathbf{w}), (\mathbf{x}', \mathbf{w}'))$  is a positive-definite kernel. Then, under the given dataset  $\{(\mathbf{x}_i, \mathbf{w}_i, y_i^{(j)})\}_{i=1}^t$ , the posterior distribution of  $f^{(j)}$  is again a GP, and its posterior mean  $\mu_t^{(j)}(\mathbf{x}, \mathbf{w})$  and posterior variance  $\sigma_t^{(j)2}(\mathbf{x}, \mathbf{w})$  are given by

$$\begin{aligned} \mu_t^{(j)}(\mathbf{x}, \mathbf{w}) &= \mathbf{k}_t^{(j)}(\mathbf{x}, \mathbf{w})^\top (\mathbf{K}_t^{(j)} + \sigma_{\text{noise}}^{(j)2} \mathbf{I}_t)^{-1} \mathbf{y}_t^{(j)}, \\ \sigma_t^{(j)2}(\mathbf{x}, \mathbf{w}) &= k^{(j)}((\mathbf{x}, \mathbf{w}), (\mathbf{x}, \mathbf{w})) - \mathbf{k}_t^{(j)}(\mathbf{x}, \mathbf{w})^\top (\mathbf{K}_t^{(j)} + \sigma_{\text{noise}}^{(j)2} \mathbf{I}_t)^{-1} \mathbf{k}_t^{(j)}(\mathbf{x}, \mathbf{w}), \end{aligned}$$

where  $\mathbf{k}_t^{(j)}(\mathbf{x}, \mathbf{w})$  is the  $t$ -dimensional vector whose  $k$ th element is  $k^{(j)}((\mathbf{x}, \mathbf{w}), (\mathbf{x}_k, \mathbf{w}_k))$ ,  $\mathbf{y}_t^{(j)} = (y_1^{(j)}, \dots, y_t^{(j)})^\top$ ,  $\mathbf{K}_t^{(j)}$  is the  $t \times t$  matrix whose  $(k, l)$ th element is  $k^{(j)}((\mathbf{x}_k, \mathbf{w}_k), (\mathbf{x}_l, \mathbf{w}_l))$  and  $\mathbf{I}_t$  is the  $t \times t$  identity matrix.

## A.2. Proposed Method in the Generalized Setting

Here, we propose a BO method for efficiently identifying  $Z_t^*$ . Using the same argument as the method used in the main body, we construct credible intervals for  $F_t^{(1)}(\mathbf{x}), \dots, F_t^{(m)}(\mathbf{x})$  using the method proposed by [Kirschner et al., 2020], and give an estimation method for the PF based on the constructed credible intervals.

### A.2.1. Composition of Credible Intervals and Pareto-frontier Estimation

For each  $(\mathbf{x}, \mathbf{w}) \in \mathcal{X} \times \Omega$ ,  $j \in [m]$  and time  $t$ , let  $Q_t^{(f^{(j)})}(\mathbf{x}, \mathbf{w}) = [l_t^{(f^{(j)})}(\mathbf{x}, \mathbf{w}), u_t^{(f^{(j)})}(\mathbf{x}, \mathbf{w})]$  be a credible interval of  $f^{(j)}(\mathbf{x}, \mathbf{w})$ . Here,  $l_t^{(f^{(j)})}(\mathbf{x}, \mathbf{w})$  and  $u_t^{(f^{(j)})}(\mathbf{x}, \mathbf{w})$  are given by

$$\begin{aligned} l_t^{(f^{(j)})}(\mathbf{x}, \mathbf{w}) &= \mu_t^{(j)}(\mathbf{x}, \mathbf{w}) - \beta_{j,t}^{1/2} \sigma_t^{(j)}(\mathbf{x}, \mathbf{w}), \\ u_t^{(f^{(j)})}(\mathbf{x}, \mathbf{w}) &= \mu_t^{(j)}(\mathbf{x}, \mathbf{w}) + \beta_{j,t}^{1/2} \sigma_t^{(j)}(\mathbf{x}, \mathbf{w}), \end{aligned}$$

where  $\beta_{j,t}^{1/2} \geq 0$ . Then, the credible interval for  $F_t^{(j)}(\mathbf{x})$  is denoted as  $Q_t^{(F_t^{(j)})}(\mathbf{x}) \equiv [l_t^{(F_t^{(j)})}(\mathbf{x}), u_t^{(F_t^{(j)})}(\mathbf{x})]$ , where its lower and upper are given by

$$\begin{aligned} l_t^{(F_t^{(j)})}(\mathbf{x}) &= \inf_{p(\mathbf{w}) \in \mathcal{A}_t} \sum_{\mathbf{w} \in \Omega} l_t^{(f^{(j)})}(\mathbf{x}, \mathbf{w}) p(\mathbf{w}), \\ u_t^{(F_t^{(j)})}(\mathbf{x}) &= \inf_{p(\mathbf{w}) \in \mathcal{A}_t} \sum_{\mathbf{w} \in \Omega} u_t^{(f^{(j)})}(\mathbf{x}, \mathbf{w}) p(\mathbf{w}). \end{aligned}$$

Next, for each  $\mathbf{x} \in \mathcal{X}$ , subset  $E \subset \mathcal{X}$  and time  $t$ , we define  $\mathbf{LCB}_t^{(m)}(\mathbf{x})$ ,  $\mathbf{UCB}_t^{(m)}(\mathbf{x})$  and  $\mathbf{LCB}_t^{(m)}(E)$  as

$$\begin{aligned} \mathbf{LCB}_t^{(m)}(\mathbf{x}) &= (l_t^{(F_t^{(1)})}(\mathbf{x}), \dots, l_t^{(F_t^{(m)})}(\mathbf{x})), \quad \mathbf{UCB}_t^{(m)}(\mathbf{x}) = (u_t^{(F_t^{(1)})}(\mathbf{x}), \dots, u_t^{(F_t^{(m)})}(\mathbf{x})), \\ \mathbf{LCB}_t^{(m)}(E) &= \{\mathbf{LCB}_t^{(m)}(\mathbf{x}) \mid \mathbf{x} \in E\}. \end{aligned}$$

Using this, we define the estimated Pareto solutions set  $\hat{\Pi}_t^{(m)} \subset \mathcal{X}$  for design variables as

$$\hat{\Pi}_t^{(m)} = \{\mathbf{x} \in \mathcal{X} \mid \mathbf{LCB}_t^{(m)}(\mathbf{x}) \in \text{Par}(\mathbf{LCB}_t^{(m)}(\mathcal{X}))\}.$$

Hereafter, for simplicity, we denote  $\mathbf{LCB}_t^{(m)}(\mathbf{x})$ ,  $\mathbf{UCB}_t^{(m)}(\mathbf{x})$ ,  $\mathbf{LCB}_t^{(m)}(E)$  and  $\hat{\Pi}_t^{(m)}$  as  $\mathbf{LCB}_t(\mathbf{x})$ ,  $\mathbf{UCB}_t(\mathbf{x})$ ,  $\mathbf{LCB}_t(E)$  and  $\hat{\Pi}_t$ , respectively.

### A.2.2. Acquisition Function

Here, we propose an AF to determine the next evaluation point. Similar to the main body, we define the AF  $a_t(\mathbf{x})$  for  $\mathbf{x} \in \mathcal{X}$  as

$$a_t(\mathbf{x}) = \text{dist}(\mathbf{UCB}_t(\mathbf{x}), \text{Dom}(\mathbf{LCB}_t(\hat{\Pi}_t))).$$

Then, the next evaluation point is selected as follows:

**Definition A.1** (For the setting in the development phase). The next design variable  $\mathbf{x}_{t+1}$  to be evaluated is selected by

$$\mathbf{x}_{t+1} = \underset{\mathbf{x} \in \mathcal{X}}{\text{argmax}} a_t(\mathbf{x}).$$

Similarly, the next environmental variable  $\mathbf{w}_{t+1}$  to be evaluated is selected by

$$\mathbf{w}_{t+1} = \underset{\mathbf{w} \in \Omega}{\text{argmax}} \{\sigma_t^{(1)2}(\mathbf{x}_{t+1}, \mathbf{w}) + \dots + \sigma_t^{(m)2}(\mathbf{x}_{t+1}, \mathbf{w})\}.$$

Notably, since  $\mathbf{w}_{t+1}$  cannot be selected in the setting at the use phase,  $\mathbf{w}_{t+1}$  is the realized value from  $P^\dagger$  at time  $t+1$ . Here,  $a_t(\mathbf{x})$  can be computed analytically by the following lemma:

**Lemma A.1.** Let  $\mathbf{UCB}_t(\mathbf{x}) = (u_1, \dots, u_m)$  and  $\mathbf{LCB}_t(\hat{\Pi}_t) = \{(l_1^{(i)}, \dots, l_m^{(i)}) \mid 1 \leq i \leq k\}$ . Then,  $a_t(\mathbf{x})$  can be computed as follows:

$$a_t(\mathbf{x}) = \max\{\tilde{a}_t(\mathbf{x}), 0\}, \quad \tilde{a}_t(\mathbf{x}) = \min_{1 \leq i \leq k} \max\{u_1 - l_1^{(i)}, \dots, u_m - l_m^{(i)}\}.$$

### A.2.3. Stopping Condition

Here, we give a stopping condition of our proposed algorithm. As in the main body, let  $\epsilon > 0$  be a user-specified stopping parameter. Then, algorithms terminate if  $a_t(\mathbf{x}) \leq \epsilon$  is satisfied. Finally, the pseudo-codes of the proposed algorithm in the development phase and use phase settings are given in Algorithm 2 and 3, respectively.

---

**Algorithm 2** BO for identifying DR-PF in the development phase setting

---

**Input:** GP prior  $\mathcal{GP}(0, k^{(j)})$ , candidate distribution family  $\mathcal{A}_t$ , tradeoff parameter  $\{\beta_{j,t}\}_{t \geq 0}$ , stopping parameter  $\epsilon > 0, j \in [m]$

$t \leftarrow 1$

**while**  $a_t(\mathbf{x}) > \epsilon$  **do**

    Compute  $Q_t^{(F_t^{(j)})}(\mathbf{x})$  for each  $\mathbf{x} \in \mathcal{X}$  and  $j \in [m]$

    Select the next evaluation point  $(\mathbf{x}_t, \mathbf{w}_t)$

    Observe  $y_t^{(j)} = f^{(j)}(\mathbf{x}_t, \mathbf{w}_t) + \varepsilon_t^{(j)}$  for each  $j \in [m]$

    Update GPs by adding observed points

$t \leftarrow t + 1$

**end while**

**Output:** Return  $\hat{\Pi}_t$  as the estimated set of design variables comprising the DR-PF

---

---

**Algorithm 3** BO for identifying DR-PF in the use phase setting

---

**Input:** GP prior  $\mathcal{GP}(0, k^{(j)})$ , candidate distribution family  $\mathcal{A}_t$ , tradeoff parameter  $\{\beta_{j,t}\}_{t \geq 0}$ , stopping parameter  $\epsilon > 0, j \in [m]$

$t \leftarrow 1$

**while**  $a_t(\mathbf{x}) > \epsilon$  **do**

    Compute  $Q_t^{(F_t^{(j)})}(\mathbf{x})$  for each  $\mathbf{x} \in \mathcal{X}$  and  $j \in [m]$

    Select the next evaluation point  $\mathbf{x}_t$

    Generate  $\mathbf{w}_t$  from  $P^\dagger$

    Observe  $y_t^{(j)} = f^{(j)}(\mathbf{x}_t, \mathbf{w}_t) + \varepsilon_t^{(j)}$  for each  $j \in [m]$

    Update GPs by adding observed points

$t \leftarrow t + 1$

**end while**

**Output:** Return  $\hat{\Pi}_t$  as the estimated set of design variables comprising the DR-PF

---

### A.3. Theoretical Analysis

Here, we give theorems on the accuracy and convergence of the proposed algorithms. First, to give theoretical guarantees, we assume that for each  $j \in [m]$ ,  $f^{(j)}$  follows GP  $\mathcal{GP}(0, k^{(j)}((\mathbf{x}, \mathbf{w}), (\mathbf{x}', \mathbf{w}')))$ . In addition, we assume that each prior variance  $k^{(j)}((\mathbf{x}, \mathbf{w}), (\mathbf{x}, \mathbf{w})) \equiv \sigma_0^{(j)2}(\mathbf{x}, \mathbf{w})$  satisfies

$$\max_{(\mathbf{x}, \mathbf{w}) \in \mathcal{X} \times \Omega} \sigma_0^{(j)2}(\mathbf{x}, \mathbf{w}) \leq 1, \quad \forall j \in [m].$$

Furthermore, let  $\kappa_T^{(j)}$  be a maximum information gain for  $f^{(j)}$  at time  $T$ . Moreover, as in the main body, we define an  $\epsilon$ -accurate Pareto region  $Z_{\epsilon,t}$  to quantify the goodness of the predicted  $\hat{\Pi}_t$  as input points that constitute the PF. For a positive number  $\epsilon$  and the  $m$ -dimensional vector  $\boldsymbol{\epsilon} = (\epsilon, \dots, \epsilon)$ , we define  $Z_{\epsilon,t}$  as

$$Z_{\epsilon,t} = \{\mathbf{y} \in \mathbb{R}^m \mid \exists \mathbf{y}' \in Z_t^* \text{ s.t. } \mathbf{y} \preceq \mathbf{y}' \text{ and } \exists \mathbf{y}'' \in Z_t^* \text{ s.t. } \mathbf{y}'' \preceq \mathbf{y} + \boldsymbol{\epsilon}\}.$$

Using  $Z_{\epsilon,t}$ , we define the accuracy of  $\hat{\Pi}_t$  as follows:

**Definition A.2** (Accuracy for  $\hat{\Pi}_t$ ). Let  $\epsilon$  be a positive number. Then, we define  $\hat{\Pi}_t$  to be an  $\epsilon$ -accurate estimated solution set if the following holds:

$$\mathbf{F}_t(\hat{\Pi}_t) \subset Z_{\epsilon,t}. \tag{A.1}$$

In addition, we define  $\hat{\Pi}_t$  to be an  $\epsilon$ -accurate estimated Pareto solution set if the following holds:

$$\text{Par}(\mathbf{F}_t(\hat{\Pi}_t)) \subset Z_{\epsilon,t}. \tag{A.2}$$

Then, the following theorem guarantees that the proposed algorithms satisfy both (A.1) and (A.2) with a high probability.

**Theorem A.1.** Let  $t \geq 1$  and  $\delta \in (0, 1)$ , and define  $\beta_{1,t} = \dots = \beta_{m,t} = 2 \log(m|\mathcal{X} \times \Omega| \pi^2 t^2 / (6\delta)) \equiv \beta_t$ . Moreover, let  $\epsilon > 0$  be a user-specified stopping parameter. Then, when Algorithm 2 terminates, with a probability of at least  $1 - \delta$ ,  $\hat{\Pi}_t$  satisfies both (A.1) and (A.2) for any  $\mathcal{A}_t$ .

Next, we give a theorem on convergence in the development phase setting. The following theorem gives convergence guarantees for Algorithm 2:

**Theorem A.2.** Under the same condition as in Theorem A.1, let  $T$  be the smallest positive integer satisfying the following inequality:

$$\frac{\beta_T(C_1\kappa_T^{(1)} + \cdots + C_m\kappa_T^{(m)})}{T} \leq \frac{\epsilon^2}{4},$$

where  $C_j = 2/\log(1 + \sigma_{\text{noise}}^{(j)-2})$  and  $j \in [m]$ . Then, Algorithm 2 terminates after at most  $T$  iterations.

Next, we give the theorem on convergence under the setting in the use phase. Unlike the setting in the development phase, we cannot control  $\mathbf{w}$  in the use phase. Therefore, to make a reasonable inference, the uncertainty at all points must be able to be reduced stochastically. However, if the value of the true probability function  $p^\dagger(\mathbf{w})$  at some  $\mathbf{w} \in \Omega$  is zero, the uncertainty of  $f^{(j)}(\mathbf{x}, \mathbf{w})$  containing this point cannot be sufficiently small. To avoid this problem, we make the following assumption on the true probability function:

$$\min_{\mathbf{w} \in \Omega} p^\dagger(\mathbf{w}) \equiv p_{\min} > 0.$$

Then, the following theorem holds:

**Theorem A.3.** Under the same condition as in Theorem A.1, assume that  $p_{\min} > 0$ . Let  $T$  be the smallest positive integer satisfying the following inequality:

$$\frac{\beta_T(\tilde{C}_1\kappa_T^{(1)} + \cdots + \tilde{C}_m\kappa_T^{(m)} + \tilde{C})}{T} \leq \frac{\epsilon^2}{4},$$

where  $\tilde{C}_j = (4p_{\min}^{-1})/\log(1 + \sigma_{\text{noise}}^{(j)-2})$ ,  $\tilde{C} = 8mp_{\min}^{-1}\log(8m/\delta)$  and  $j \in [m]$ . Then, with a probability of at least  $1 - \delta$ , Algorithm 3 terminates after at most  $T$  trials.

Finally, we show that under appropriate assumptions, the solution to the distributionally robust Pareto optimization problem is also a good solution to the Pareto optimization problem defined by the true expectation in the use phase setting. Here, the expectation function  $\tilde{F}^{(j)}(\mathbf{x})$  determined by the true probability function  $p^\dagger(\mathbf{w})$  is given by

$$\tilde{F}^{(j)}(\mathbf{x}) = \sum_{\mathbf{w} \in \Omega} f^{(j)}(\mathbf{x}, \mathbf{w})p^\dagger(\mathbf{w}), \quad j \in [m].$$

In addition, for each  $\mathbf{x} \in \mathcal{X}$  and  $E \subset \mathcal{X}$ , let  $\tilde{\mathbf{F}}(\mathbf{x}) = (\tilde{F}^{(1)}(\mathbf{x}), \dots, \tilde{F}^{(m)}(\mathbf{x}))$  and  $\tilde{\mathbf{F}}(E) = \{\tilde{\mathbf{F}}(\mathbf{x}) \mid \mathbf{x} \in E\}$ . Then, the PF  $\tilde{Z}^*$  defined by  $\tilde{F}^{(1)}(\mathbf{x}), \dots, \tilde{F}^{(m)}(\mathbf{x})$  can be expressed as follows:

$$\tilde{Z}^* = \text{Par}(\tilde{\mathbf{F}}(\mathcal{X})).$$

Furthermore, as in the case of  $Z_t^*$ , we define an  $\epsilon$ -accurate Pareto region  $\tilde{Z}_\epsilon$  for  $\tilde{Z}^*$ . For a positive number  $\epsilon$  and an  $m$ -dimensional vector  $\boldsymbol{\epsilon} = (\epsilon, \dots, \epsilon)$ , we define  $\tilde{Z}_\epsilon$  as

$$\tilde{Z}_\epsilon = \{\mathbf{y} \in \mathbb{R}^m \mid \exists \mathbf{y}' \in \tilde{Z}^* \text{ s.t. } \mathbf{y} \preceq \mathbf{y}' \text{ and } \exists \mathbf{y}'' \in \tilde{Z}^* \text{ s.t. } \mathbf{y}'' \preceq \mathbf{y} + \boldsymbol{\epsilon}\}.$$

Using  $\tilde{Z}_\epsilon$ , we define the accuracy of  $\hat{\Pi}_t$  for  $\tilde{Z}^*$ .

**Definition A.3** (Accuracy of  $\hat{\Pi}_t$  for  $\tilde{Z}^*$ ). Let  $\epsilon$  be a positive number. Then, we define  $\hat{\Pi}_t$  to be an  $\epsilon$ -accurate estimated solution set for  $\tilde{Z}^*$  if the following holds:

$$\mathbf{F}_t(\hat{\Pi}_t) \subset \tilde{Z}_\epsilon.$$

Moreover, we define  $\hat{\Pi}_t$  to be an  $\epsilon$ -accurate estimated Pareto solution set for  $\tilde{Z}^*$  if the following holds:

$$\text{Par}(\mathbf{F}_t(\hat{\Pi}_t)) \subset \tilde{Z}_\epsilon.$$

Then, the following theorem holds:

**Theorem A.4.** Under the use phase setting, let  $t \geq 1$  and  $\delta \in (0, 1)$ , and define  $\beta_{1,t} = \cdots = \beta_{m,t} = 2\log(m|\mathcal{X} \times \Omega|\pi^2 t^2)/(6\delta) \equiv \beta_t$ . Moreover, let  $\epsilon > 0$  be a user-specified stopping parameter. Furthermore, let the reference distribution  $p_t^*(\mathbf{w})$  be the empirical distribution function for  $\mathbf{w}$ , and define  $\xi_t$  and the distance between distributions  $d(\cdot, \cdot)$  as

$$\xi_t = |\Omega| \sqrt{\frac{1}{2t} \log \left( \frac{|\Omega|\pi^2 t^2}{3\delta} \right)},$$

$$d(p_1(\mathbf{w}), p_2(\mathbf{w})) = \sum_{\mathbf{w} \in \Omega} |p_1(\mathbf{w}) - p_2(\mathbf{w})|.$$

Then, if Algorithm 3 terminates at  $t \geq T$  after time  $T$ , with a probability of at least  $1 - 2\delta$ ,  $\hat{\Pi}_t$  is the  $2\epsilon$ -accurate estimated set and estimated Pareto set, that is, the following holds:

$$\mathbf{F}_t(\hat{\Pi}_t) \subset \tilde{Z}_{2\epsilon}, \quad \text{Par}(\mathbf{F}_t(\hat{\Pi}_t)) \subset \tilde{Z}_{2\epsilon}.$$

Here,  $T$  is the smallest positive integer satisfying the following inequality:

$$\forall n \geq T, 2\beta_1^{1/2}\xi_n \leq \epsilon. \tag{A.3}$$

## B. Proofs

Here, we give proofs of Lemma A.1 and Theorem A.1–A.4. Notably, Lemma 3.1 and Theorem 4.1–4.2 in the main body are special cases of Lemma A.1 and Theorem A.1–A.2, respectively. First, we prove Lemma A.1.

**Proof.** Let  $\mathbf{UCB}_t(\mathbf{x}) = (u_1, \dots, u_m) \equiv \mathbf{u}$  and  $\mathbf{LCB}_t(\hat{\Pi}_t) = \{(l_1^{(i)}, \dots, l_m^{(i)}) \mid 1 \leq i \leq k\} \equiv \mathcal{L}$ . Here, if  $\mathbf{u} \in \text{Dom}(\mathcal{L})$ , then the following holds from the definition of  $\text{dist}(\mathbf{a}, B)$ :

$$a_t(\mathbf{x}) = \text{dist}(\mathbf{u}, \text{Dom}(\mathcal{L})) = \inf_{\mathbf{b} \in \text{Dom}(\mathcal{L})} d_\infty(\mathbf{u}, \mathbf{b}) = d_\infty(\mathbf{u}, \mathbf{u}) = 0.$$

In addition, since  $\mathbf{u} \in \text{Dom}(\mathcal{L})$ , there exists  $(l_1^{(i)}, \dots, l_m^{(i)})$  such that  $u_j \leq l_j^{(i)}$  for any  $j \in [m]$ . Thus, we have  $\max\{u_1 - l_1^{(i)}, \dots, u_m - l_m^{(i)}\} \leq 0$ . This implies that

$$\tilde{a}_t(\mathbf{x}) = \min_{1 \leq i \leq k} \max\{u_1 - l_1^{(i)}, \dots, u_m - l_m^{(i)}\} \leq 0$$

and  $\max\{\tilde{a}_t(\mathbf{x}), 0\} = 0$ . Therefore, we get  $a_t(\mathbf{x}) = \max\{\tilde{a}_t(\mathbf{x}), 0\}$ . Next, we consider the case where  $\mathbf{u} \notin \text{Dom}(\mathcal{L})$ . Let  $a_t(\mathbf{x}) = \eta$ . Then, noting that  $\mathbf{u} \notin \text{Dom}(\mathcal{L})$ , for any  $i \in \{1, \dots, k\}$ , there exists  $j \in [m]$  such that  $u_j > l_j^{(i)}$ . This implies that

$$\tilde{a}_t(\mathbf{x}) = \min_{1 \leq i \leq k} \max\{u_1 - l_1^{(i)}, \dots, u_m - l_m^{(i)}\} \equiv \tilde{\eta} > 0$$

and  $\max\{\tilde{a}_t(\mathbf{x}), 0\} = \tilde{a}_t(\mathbf{x}) = \tilde{\eta}$ . For this  $\tilde{\eta}$ , there exists  $i$  such that

$$u_j - l_j^{(i)} \leq \tilde{\eta} \quad \forall j \in [m].$$

Hence, we have  $\tilde{\mathbf{u}} \equiv (u_1 - \tilde{\eta}, \dots, u_m - \tilde{\eta}) \in \text{Dom}(\mathcal{L})$  because  $u_j - \tilde{\eta} \leq l_j^{(i)}$  for any  $j \in [m]$ . Thus, from the definition of  $a_t(\mathbf{x})$ , the following holds:

$$\eta = a_t(\mathbf{x}) = \text{dist}(\mathbf{u}, \text{Dom}(\mathcal{L})) = \inf_{\mathbf{b} \in \text{Dom}(\mathcal{L})} d_\infty(\mathbf{u}, \mathbf{b}) \leq d_\infty(\mathbf{u}, \tilde{\mathbf{u}}) = \tilde{\eta}.$$

Here, we assume  $\eta < \tilde{\eta}$ . Then, noting that  $\text{Dom}(\mathcal{L})$  is the closed set, there exists  $\tilde{\mathbf{l}} = (\tilde{l}_1, \dots, \tilde{l}_m) \in \text{Dom}(\mathcal{L})$  such that  $d_\infty(\mathbf{u}, \tilde{\mathbf{l}}) = \eta$ . Therefore,  $\tilde{\mathbf{l}}$  can be expressed as  $\tilde{\mathbf{l}} = (u_1 - s_1, \dots, u_m - s_m)$ , where  $0 \leq |s_j| \leq \eta$  and at least one of  $s_1, \dots, s_m$  is  $\eta$ . Thus, since  $(u_1 - \eta, \dots, u_m - \eta) \preceq \tilde{\mathbf{l}}$ , noting that  $(u_1 - \eta, \dots, u_m - \eta) \in \text{Dom}(\mathcal{L})$  there exists  $i$  such that

$$u_j - \eta \leq l_j^{(i)} \quad \forall j \in [m].$$

This implies that  $\max\{u_1 - l_1^{(i)}, \dots, u_m - l_m^{(i)}\} \leq \eta$ . Hence, it follows that

$$\tilde{\eta} = \min_{1 \leq i \leq k} \max\{u_1 - l_1^{(i)}, \dots, u_m - l_m^{(i)}\} \leq \eta.$$

However, this is a contradiction with  $\eta < \tilde{\eta}$ . Consequently, we obtain  $a_t(\mathbf{x}) = \max\{\tilde{a}_t(\mathbf{x}), 0\}$ .  $\square$

Next, we prove Theorem A.1.

**Proof.** First, we prove  $\mathbf{F}_t(\hat{\Pi}_t) \subset Z_{\epsilon, t}$ . Since  $\hat{\Pi}_t \subset \mathcal{X}$ , for any  $\mathbf{y} \in \mathbf{F}_t(\hat{\Pi}_t)$ , there exists  $\mathbf{y}' \in Z_t^*$  such that  $\mathbf{y} \preceq \mathbf{y}'$ . Thus, it is sufficient to show that there exists  $\mathbf{y}'' \in Z_t^*$  such that  $\mathbf{y}'' \preceq \mathbf{y} + \epsilon$ . Here, under the theorem's assumption, with a probability of at least  $1 - \delta$ , the following holds for any  $(\mathbf{x}, \mathbf{w}) \in \mathcal{X} \times \Omega$ ,  $j \in [m]$  and time  $t \geq 1$ :

$$f^{(j)}(\mathbf{x}, \mathbf{w}) \in Q_t^{(f^{(j)})}(\mathbf{x}, \mathbf{w}),$$

where this relation can be derived by using Lemma 5.1 of [Srinivas et al., 2010]. Hence, we have  $F_t^{(j)}(\mathbf{x}) \in Q_t^{(F_t^{(j)})}(\mathbf{x})$ . In addition, since  $Z_t^*$  is the closed set, for any  $\mathbf{x} \in \hat{\Pi}_t$ , there exist  $a \geq 0$  and  $\mathbf{F}_t(\mathbf{x}) + (a, \dots, a) \equiv \mathbf{y}'' \in Z_t^*$  such that

$$\text{dist}(\mathbf{F}_t(\mathbf{x}), Z_t^*) = d_\infty(\mathbf{F}_t(\mathbf{x}), \mathbf{y}'') \leq d_\infty((l_t^{(F_t^{(1)})}(\mathbf{x}), \dots, l_t^{(F_t^{(m)})}(\mathbf{x})), \mathbf{y}'''),$$

where  $\mathbf{y}''' \in Z_t^*$  can be given by using  $s \geq a \geq 0$  as  $\mathbf{y}''' = (l_t^{(F_t^{(1)})}(\mathbf{x}), \dots, l_t^{(F_t^{(m)})}(\mathbf{x})) + (s, \dots, s)$ . Here, for some  $\hat{\mathbf{x}} \in \mathcal{X}$  satisfying  $\mathbf{y}''' \preceq \mathbf{F}_t(\hat{\mathbf{x}})$ , the following holds:

$$d_\infty((l_t^{(F_t^{(1)})}(\mathbf{x}), \dots, l_t^{(F_t^{(m)})}(\mathbf{x})), \mathbf{y}''') \leq \text{dist}(\mathbf{F}_t(\hat{\mathbf{x}}), \text{Dom}(\mathbf{LCB}_t(\hat{\Pi}_t))).$$

Moreover, the right hand side is bounded from above as

$$\begin{aligned} & \text{dist}(\mathbf{F}_t(\hat{\mathbf{x}}), \text{Dom}(\mathbf{LCB}_t(\hat{\Pi}_t))) \\ & \leq \text{dist}(\mathbf{UCB}_t(\hat{\mathbf{x}}), \text{Dom}(\mathbf{LCB}_t(\hat{\Pi}_t))) \\ & \leq \max_{\mathbf{x}^\dagger \in \mathcal{X}} \text{dist}(\mathbf{UCB}_t(\mathbf{x}^\dagger), \text{Dom}(\mathbf{LCB}_t(\hat{\Pi}_t))) = a_t(\mathbf{x}_{t+1}). \end{aligned}$$

Therefore, if  $a_t(\mathbf{x}_{t+1}) \leq \epsilon$ , then  $d_\infty(\mathbf{F}_t(\mathbf{x}), \mathbf{y}'') \leq \epsilon$ . It follows that  $\mathbf{y}'' \preceq \mathbf{F}_t(\mathbf{x}) + \epsilon$ . Since  $\mathbf{x}$  is an arbitrary element of  $\hat{\Pi}_t$ , we have  $\mathbf{F}_t(\hat{\Pi}_t) \subset Z_{\epsilon,t}$ . Next, we prove  $\text{Par}(\mathbf{F}_t(\hat{\Pi}_t)) \subset Z_{\epsilon,t}$ . As before, noting that  $\hat{\Pi}_t \subset \mathcal{X}$ , for any  $\mathbf{y} \in \text{Par}(\mathbf{F}_t(\hat{\Pi}_t))$ , there exists  $\mathbf{y}' \in Z_t^*$  such that  $\mathbf{y} \preceq \mathbf{y}'$ . In addition, since  $Z_t^*$  is the closed set, for any  $\mathbf{y} \in \text{Par}(\mathbf{F}_t(\hat{\Pi}_t))$ , there exist  $a \geq 0$  and  $\mathbf{y} + (a, \dots, a) \equiv \mathbf{y}'' \in Z_t^*$  such that

$$\text{dist}(\mathbf{y}, Z_t^*) = d_\infty(\mathbf{y}, \mathbf{y}'').$$

Here, for some  $\hat{\mathbf{x}} \in \mathcal{X}$  satisfying  $\mathbf{y}'' \preceq \mathbf{F}_t(\hat{\mathbf{x}})$ , the following holds:

$$d_\infty(\mathbf{y}, \mathbf{y}'') \leq d_\infty(\mathbf{y}'', \mathbf{F}_t(\hat{\mathbf{x}})) \leq \text{dist}(\mathbf{F}_t(\hat{\mathbf{x}}), \text{Dom}(\mathbf{LCB}_t(\hat{\Pi}_t))),$$

where  $\mathbf{y}''' \in \text{Par}(\mathbf{F}_t(\hat{\Pi}_t))$  can be given by using  $s' \geq a \geq 0$  as  $\mathbf{y}''' = \mathbf{F}_t(\hat{\mathbf{x}}) - (s', \dots, s')$ . Then, we obtain

$$\begin{aligned} & \text{dist}(\mathbf{F}_t(\hat{\mathbf{x}}), \text{Dom}(\mathbf{LCB}_t(\hat{\Pi}_t))) \\ & \leq \text{dist}(\mathbf{UCB}_t(\hat{\mathbf{x}}), \text{Dom}(\mathbf{LCB}_t(\hat{\Pi}_t))) \\ & \leq \max_{\mathbf{x}^\dagger \in \mathcal{X}} \text{dist}(\mathbf{UCB}_t(\mathbf{x}^\dagger), \text{Dom}(\mathbf{LCB}_t(\hat{\Pi}_t))) = a_t(\mathbf{x}_{t+1}). \end{aligned}$$

Thus, if  $a_t(\mathbf{x}_{t+1}) \leq \epsilon$ , then  $d_\infty(\mathbf{y}, \mathbf{y}'') \leq \epsilon$ . This implies that  $\mathbf{y}'' \preceq \mathbf{y} + \epsilon$ . Consequently, since  $\mathbf{y}$  is an arbitrary element of  $\text{Par}(\mathbf{F}_t(\hat{\Pi}_t))$ , we have  $\text{Par}(\mathbf{F}_t(\hat{\Pi}_t)) \subset Z_{\epsilon,t}$ .  $\square$

Next, we prove Theorem A.2.

**Proof.** Let  $\mathbf{x}_t = \text{argmax}_{\mathbf{x} \in \mathcal{X}} a_{t-1}(\mathbf{x})$ . Here, since  $\mathbf{LCB}_{t-1}(\mathbf{x}_t) \in \text{Dom}(\mathbf{LCB}_{t-1}(\hat{\Pi}_{t-1}))$ , the following inequality holds:

$$\begin{aligned} a_{t-1}(\mathbf{x}_t) &= \text{dist}(\mathbf{UCB}_{t-1}(\mathbf{x}_t), \text{Dom}(\mathbf{LCB}_{t-1}(\hat{\Pi}_{t-1}))) \\ &\leq d_\infty(\mathbf{UCB}_{t-1}(\mathbf{x}_t), \mathbf{LCB}_{t-1}(\mathbf{x}_t)) \\ &= \max_{1 \leq j \leq m} \{u_{t-1}^{(F_{t-1}^{(j)})}(\mathbf{x}_t) - l_{t-1}^{(F_{t-1}^{(j)})}(\mathbf{x}_t)\}. \end{aligned}$$

Therefore, from the definition of  $u_{t-1}^{(F_{t-1}^{(j)})}(\mathbf{x}_t)$  and  $l_{t-1}^{(F_{t-1}^{(j)})}(\mathbf{x}_t)$ , we get

$$u_{t-1}^{(F_{t-1}^{(j)})}(\mathbf{x}_t) - l_{t-1}^{(F_{t-1}^{(j)})}(\mathbf{x}_t) \leq 2\beta_t^{1/2} \max_{\mathbf{w} \in \Omega} \sigma_{t-1}^{(j)}(\mathbf{x}_t, \mathbf{w}).$$

Hence, the following inequality holds:

$$a_{t-1}^2(\mathbf{x}_t) \leq 4\beta_t \max_{1 \leq j \leq m} \max_{\mathbf{w} \in \Omega} \sigma_{t-1}^{(j)2}(\mathbf{x}_t, \mathbf{w}).$$

Furthermore, since  $\mathbf{w}_t$  is selected by

$$\mathbf{w}_t = \text{argmax}_{\mathbf{w} \in \Omega} (\sigma_{t-1}^{(1)2}(\mathbf{x}_t, \mathbf{w}) + \dots + \sigma_{t-1}^{(m)2}(\mathbf{x}_t, \mathbf{w})),$$

the following holds:

$$\begin{aligned} a_{t-1}^2(\mathbf{x}_t) &\leq 4\beta_t \max_{1 \leq j \leq m} \max_{\mathbf{w} \in \Omega} \sigma_{t-1}^{(j)2}(\mathbf{x}_t, \mathbf{w}) \\ &\leq 4\beta_t (\sigma_{t-1}^{(1)2}(\mathbf{x}_t, \mathbf{w}_t) + \dots + \sigma_{t-1}^{(m)2}(\mathbf{x}_t, \mathbf{w}_t)). \end{aligned}$$

In addition, let  $T$  be the number given by Theorem A.2. Then, we get

$$\begin{aligned} T \min_{1 \leq t \leq T} a_{t-1}^2(\mathbf{x}_t) &\leq \sum_{t=1}^T a_{t-1}^2(\mathbf{x}_t) \\ &\leq 4\beta_T \sum_{j=1}^m \sum_{t=1}^T \sigma_{t-1}^{(j)2}(\mathbf{x}_t, \mathbf{w}_t) \\ &\leq 4\beta_T (C_1 \kappa_T^{(1)} + \dots + C_m \kappa_T^{(m)}), \end{aligned}$$



where the last inequality can be derived by using Lemma 5.3 and 5.4 of [Srinivas et al., 2010]. Therefore, dividing both sides by  $T$ , we obtain

$$\min_{1 \leq t \leq T} a_{t-1}^2(\mathbf{x}_t) \leq 4\beta_T \frac{C_1 \kappa_T^{(1)} + \dots + C_m \kappa_T^{(m)}}{T} \leq \epsilon^2.$$

Hence, we get  $\min_{1 \leq t \leq T} a_{t-1}(\mathbf{x}_t) \leq \epsilon$ . This implies that there exists  $t' \in \{1, \dots, T\}$  such that  $a_{t'-1}(\mathbf{x}_{t'}) \leq \epsilon$ .  $\square$

Next, we prove Theorem A.3.

**Proof.** Using the same argument as in the proof of Theorem A.2, we have

$$a_{t-1}^2(\mathbf{x}_t) \leq 4\beta_t \max_{1 \leq j \leq m} \max_{\mathbf{w} \in \Omega} \sigma_{t-1}^{(j)2}(\mathbf{x}_t, \mathbf{w}).$$

Furthermore, since  $p_{\min} > 0$ , the following inequality holds:

$$\begin{aligned} \max_{\mathbf{w} \in \Omega} \sigma_{t-1}^{(j)2}(\mathbf{x}_t, \mathbf{w}) &\leq \sum_{\mathbf{w} \in \Omega} \sigma_{t-1}^{(j)2}(\mathbf{x}_t, \mathbf{w}) \\ &= \sum_{\mathbf{w} \in \Omega} (p^\dagger(\mathbf{w}))^{-1} p^\dagger(\mathbf{w}) \sigma_{t-1}^{(j)2}(\mathbf{x}_t, \mathbf{w}) \\ &\leq p_{\min}^{-1} \sum_{\mathbf{w} \in \Omega} p^\dagger(\mathbf{w}) \sigma_{t-1}^{(j)2}(\mathbf{x}_t, \mathbf{w}) \\ &\equiv p_{\min}^{-1} \mathbb{E}_{\mathbf{w}}[\sigma_{t-1}^{(j)2}(\mathbf{x}_t, \mathbf{w})]. \end{aligned}$$

Using this, we get

$$\begin{aligned} \max_{1 \leq j \leq m} \max_{\mathbf{w} \in \Omega} \sigma_{t-1}^{(j)2}(\mathbf{x}_t, \mathbf{w}) &\leq \sum_{j=1}^m \max_{\mathbf{w} \in \Omega} \sigma_{t-1}^{(j)2}(\mathbf{x}_t, \mathbf{w}) \\ &\leq p_{\min}^{-1} \sum_{j=1}^m \mathbb{E}_{\mathbf{w}}[\sigma_{t-1}^{(j)2}(\mathbf{x}_t, \mathbf{w})] \\ &= p_{\min}^{-1} \mathbb{E}_{\mathbf{w}} \left[ \sum_{j=1}^m \sigma_{t-1}^{(j)2}(\mathbf{x}_t, \mathbf{w}) \right]. \end{aligned}$$

Here, let  $T$  be the number given by Theorem A.3. Then, we obtain

$$\begin{aligned} T \min_{1 \leq t \leq T} a_{t-1}^2(\mathbf{x}_t) &\leq \sum_{t=1}^T a_{t-1}^2(\mathbf{x}_t) \\ &\leq 4\beta_T p_{\min}^{-1} \sum_{t=1}^T \mathbb{E}_{\mathbf{w}} \left[ \sum_{j=1}^m \sigma_{t-1}^{(j)2}(\mathbf{x}_t, \mathbf{w}) \right]. \end{aligned} \tag{B.1}$$

Noting that  $\sum_{j=1}^m \sigma_{t-1}^{(j)2}(\mathbf{x}_t, \mathbf{w})$  is a non-negative random variable and  $\sum_{j=1}^m \sigma_{t-1}^{(j)2}(\mathbf{x}_t, \mathbf{w}) \leq m$ , from Lemma 3 of [Kirschner and Krause, 2018], the following holds with a probability of at least  $1 - \delta$ :

$$\sum_{t=1}^T \mathbb{E}_{\mathbf{w}} \left[ \sum_{j=1}^m \sigma_{t-1}^{(j)2}(\mathbf{x}_t, \mathbf{w}) \right] \leq 2 \sum_{j=1}^m \sum_{t=1}^T \sigma_{t-1}^{(j)2}(\mathbf{x}_t, \mathbf{w}) + 4m \log \frac{1}{\delta} + 8m \log 4m + 1.$$

Moreover, since  $4m \log \frac{1}{\delta} \leq 8m \log \frac{1}{\delta}$  and  $1 \leq 8m \log 2$ , we have

$$\begin{aligned} 4m \log \frac{1}{\delta} + 8m \log 4m + 1 &\leq 8m \log \frac{1}{\delta} + 8m \log 4m + 8m \log 2 \\ &= 8m \log \frac{8m}{\delta} \end{aligned}$$

and

$$\sum_{t=1}^T \mathbb{E}_{\mathbf{w}} \left[ \sum_{j=1}^m \sigma_{t-1}^{(j)2}(\mathbf{x}_t, \mathbf{w}) \right] \leq 2 \sum_{j=1}^m \sum_{t=1}^T \sigma_{t-1}^{(j)2}(\mathbf{x}_t, \mathbf{w}) + 8m \log \frac{8m}{\delta}. \tag{B.2}$$

Hence, by substituting (B.2) into (B.1), from Lemma 5.3 and 5.4 of [Srinivas et al., 2010], we get

$$T \min_{1 \leq t \leq T} a_{t-1}^2(\mathbf{x}_t) \leq 4\beta_T(\tilde{C}_1\kappa_T^{(1)} + \cdots + \tilde{C}_m\kappa_T^{(m)} + \tilde{C}).$$

Therefore, from the definition of  $T$ , dividing both sides by  $T$ , we obtain

$$\min_{1 \leq t \leq T} a_{t-1}^2(\mathbf{x}_t) \leq 4\beta_T \frac{\tilde{C}_1\kappa_T^{(1)} + \cdots + \tilde{C}_m\kappa_T^{(m)} + \tilde{C}}{T} \leq \epsilon^2.$$

Thus, we get  $\min_{1 \leq t \leq T} a_{t-1}(\mathbf{x}_t) \leq \epsilon$ . This implies that there exists  $t' \in \{1, \dots, T\}$  such that  $a_{t'-1}(\mathbf{x}_{t'}) \leq \epsilon$ .  $\square$

Finally, we prove Theorem A.4.

**Proof.** Suppose that  $p_t^*(\mathbf{w})$  is the empirical distribution function of  $\mathbf{w}$ . Then, from Hoeffding's inequality, the following inequality holds for any  $\mathbf{w}$ :

$$\mathbb{P}(|p_t^*(\mathbf{w}) - p^\dagger(\mathbf{w})| \geq \lambda) \leq 2\exp(-2t\lambda^2).$$

Here, let

$$\lambda = \sqrt{\frac{1}{2t} \log\left(\frac{|\Omega|\pi^2 t^2}{3\delta}\right)}.$$

Then, with a probability of at least  $1 - \delta$ , the following holds for any  $t \geq 1$  and  $\mathbf{w} \in \Omega$ :

$$|p_t^*(\mathbf{w}) - p^\dagger(\mathbf{w})| \leq \lambda.$$

In addition, from the definition of  $d(\cdot, \cdot)$ , we get

$$d(p_t^*(\mathbf{w}), p^\dagger(\mathbf{w})) = \sum_{\mathbf{w} \in \Omega} |p_t^*(\mathbf{w}) - p^\dagger(\mathbf{w})| \leq |\Omega|\lambda = \xi_t.$$

This implies that  $p^\dagger(\mathbf{w}) \in \mathcal{A}_t$ . Furthermore, from the definition of  $\tilde{F}^{(j)}(\mathbf{x})$  and  $F_t^{(j)}(\mathbf{x})$ , the following inequality holds for any  $t \geq 1$ ,  $j \in [m]$  and  $\mathbf{x} \in \mathcal{X}$ :

$$F_t^{(j)}(\mathbf{x}) \leq \tilde{F}^{(j)}(\mathbf{x}).$$

Therefore, it follows that

$$\mathbf{F}_t(\mathbf{x}) \leq \tilde{\mathbf{F}}(\mathbf{x}) \quad \forall \mathbf{x} \in \mathcal{X}, \forall t \geq 1. \quad (\text{B.3})$$

Here, for any  $\mathbf{x} \in \mathcal{X}$ ,  $t \geq 1$  and  $j \in [m]$ , let  $\bar{p}_{t,\mathbf{x}}^{(j)}(\mathbf{w}) \in \mathcal{A}_t$  be the probability function satisfying

$$F_t^{(j)}(\mathbf{x}) = \sum_{\mathbf{w} \in \Omega} f^{(j)}(\mathbf{x}, \mathbf{w}) \bar{p}_{t,\mathbf{x}}^{(j)}(\mathbf{w}).$$

Then, the following inequality holds:

$$|\tilde{F}^{(j)}(\mathbf{x}) - F_t^{(j)}(\mathbf{x})| \leq \sum_{\mathbf{w} \in \Omega} |f^{(j)}(\mathbf{x}, \mathbf{w})| |p^\dagger(\mathbf{w}) - \bar{p}_{t,\mathbf{x}}^{(j)}(\mathbf{w})|.$$

Moreover, from Lemma 5.1 of [Srinivas et al., 2010], with a probability of at least  $1 - \delta$ , the following holds for any  $\mathbf{x} \in \mathcal{X}$ ,  $\mathbf{w} \in \Omega$  and  $j \in [m]$ :

$$|f^{(j)}(\mathbf{x}, \mathbf{w})| \leq \beta_1^{1/2} \sigma_0^{(j)}(\mathbf{x}, \mathbf{w}) \leq \beta_1^{1/2}.$$

Hence, we have

$$\begin{aligned} \tilde{F}^{(j)}(\mathbf{x}) - F_t^{(j)}(\mathbf{x}) &\leq |\tilde{F}^{(j)}(\mathbf{x}) - F_t^{(j)}(\mathbf{x})| \\ &\leq \beta_1^{1/2} \sum_{\mathbf{w} \in \Omega} |p^\dagger(\mathbf{w}) - \bar{p}_{t,\mathbf{x}}^{(j)}(\mathbf{w})| \\ &= \beta_1^{1/2} d(p^\dagger(\mathbf{w}), \bar{p}_{t,\mathbf{x}}^{(j)}(\mathbf{w})) \\ &\leq \beta_1^{1/2} (d(p^\dagger(\mathbf{w}), p_t^*(\mathbf{w})) + d(p_t^*(\mathbf{w}), \bar{p}_{t,\mathbf{x}}^{(j)}(\mathbf{w}))) \leq 2\beta_1^{1/2} \xi_t. \end{aligned}$$

In addition, let  $T$  be the smallest positive integer satisfying (A.3). Then, for any  $t \geq T$ , the following inequality holds:

$$\tilde{F}^{(j)}(\mathbf{x}) \leq F_t^{(j)}(\mathbf{x}) + \epsilon.$$

Thus, we obtain

$$\tilde{\mathbf{F}}(x) \preceq \mathbf{F}_t(x) + \epsilon \quad \forall x \in \mathcal{X}, \forall t \geq T. \quad (\text{B.4})$$

Therefore, by combining (B.3) and (B.4), we have

$$\text{Par}(\mathbf{F}_t(\mathcal{X})) \subset \tilde{Z}_\epsilon \quad \forall t \geq T. \quad (\text{B.5})$$

Finally, from Theorem A.1, the following holds at  $t'$ , the time at which the algorithm terminates:

$$\mathbf{F}_{t'}(\hat{\Pi}_{t'}) \subset Z_{\epsilon, t'}, \text{Par}(\mathbf{F}_{t'}(\hat{\Pi}_{t'})) \subset Z_{\epsilon, t'}. \quad (\text{B.6})$$

Consequently, if  $t' \geq T$ , using (B.5) and (B.6) we get

$$\mathbf{F}_{t'}(\hat{\Pi}_{t'}) \subset \tilde{Z}_{2\epsilon}, \text{Par}(\mathbf{F}_{t'}(\hat{\Pi}_{t'})) \subset \tilde{Z}_{2\epsilon}.$$

□

### C. Experimental Details and Additional Experiments

Here, we give experimental details and additional experiments in Section 5.

**Experimental Setup** The experimental parameters used in each experiment are described in Table 2.

Table 2: Experimental parameters for each setting

	Parameters
Simulator setting	$\sigma_{f,1}^2 = 1000, L_1 = 2, \sigma_{\text{noise}}^{(1)2} = 10^{-4}, \beta_{1,t}^{1/2} = 3, \sigma_{f,2}^2 = 1000, L_2 = 2, \sigma_{\text{noise}}^{(2)2} = 10^{-4}, \beta_{2,t}^{1/2} = 3, \xi = 0.05$
Uncontrollable setting	$\sigma_{f,1}^2 = 1000, L_1 = 2, \sigma_{\text{noise}}^{(1)2} = 10^{-4}, \beta_{1,t}^{1/2} = 3, \sigma_{f,2}^2 = 1000, L_2 = 2, \sigma_{\text{noise}}^{(2)2} = 10^{-4}, \beta_{2,t}^{1/2} = 3, \xi = 0.05$
SIR (Case1)	$\sigma_{f,1}^2 = 5000, L_1 = 0.1, \sigma_{\text{noise}}^{(1)2} = 10^{-8}, \beta_{1,t}^{1/2} = 3, \sigma_{f,2}^2 = 10^5, L_2 = 0.01, \sigma_{\text{noise}}^{(2)2} = 10^{-4}, \beta_{2,t}^{1/2} = 2, \xi = 0.15$
SIR (Case2)	$\sigma_{f,1}^2 = 10^4, L_1 = 0.1, \sigma_{\text{noise}}^{(1)2} = 10^{-3}, \beta_{1,t}^{1/2} = 2, \sigma_{f,2}^2 = 10^5, L_2 = 0.1, \sigma_{\text{noise}}^{(2)2} = 10^{-3}, \beta_{2,t}^{1/2} = 3, \xi = 0.15$

**MVA** The **MVA** method is based on reducing the uncertainty in the potential optimal set  $M_t$  and the estimated PF solution set  $\hat{\Pi}_t$ . Using  $\hat{\Pi}_t$ ,  $M_t$  is defined as follows:

$$M_t = \{x \in \mathcal{X} \setminus \hat{\Pi}_t \mid \forall x' \in \hat{\Pi}_t, u_t^{(F^{(1)})}(x) > l_t^{(F^{(1)})}(x') \text{ or } u_t^{(F^{(2)})}(x) > l_t^{(F^{(2)})}(x')\}.$$

The uncertainty  $\lambda_t(x)$  is given by

$$\lambda_t(x) = \sqrt{(u_t^{(F^{(1)})}(x) - l_t^{(F^{(1)})}(x))^2 + (u_t^{(F^{(2)})}(x) - l_t^{(F^{(2)})}(x))^2}.$$

**EHI** The **EHI** method is based on the expected hypervolume improvement for a bounded region defined by PFs and reference points. Let  $B \subset \mathbb{R}^2$  be a set, and let  $\mathbf{r} = (r_1, r_2) \in \mathbb{R}^2$  be a reference point satisfying  $\mathbf{r} \preceq B$ . Then, let us denote the bounded region dominated by  $B$  and  $\mathbf{r}$ , by

$$\text{Dom}(B; \mathbf{r}) = \text{Dom}(B) \cap [r_1, \infty) \times [r_2, \infty).$$

In **EHI**, for each  $j \in \{1, 2\}$  we calculated the estimated value of  $F^{(j)}(x)$  by using posterior means as

$$\mu_t^{(F^{(j)})}(x) = \inf_{p(w) \in \mathcal{A}} \sum_{w \in \Omega} \mu_t^{(j)}(x, w) p(w).$$

For a point  $x \in \mathcal{X}$  a subset  $E \subset \mathcal{X}$ , we define  $\boldsymbol{\mu}_t^{(\mathbf{F})}(x)$  and  $\boldsymbol{\mu}_t^{(\mathbf{F})}(E)$  as

$$\boldsymbol{\mu}_t^{(\mathbf{F})}(x) = (\mu_t^{(F^{(1)})}(x), \mu_t^{(F^{(2)})}(x)), \quad \boldsymbol{\mu}_t^{(\mathbf{F})}(E) = \{\boldsymbol{\mu}_t^{(\mathbf{F})}(x) \mid x \in E\}.$$

In our experiments, we defined the reference point  $\mathbf{r}_t = (r_{t,1}, r_{t,2})$  for each iteration  $t$  as

$$r_{t,1} = \min_{x \in \mathcal{X}} \mu_t^{(F^{(1)})}(x), \quad r_{t,2} = \min_{x \in \mathcal{X}} \mu_t^{(F^{(2)})}(x).$$

Then, the expected hypervolume improvement for  $x \in \mathcal{X}$  is given by

$$\text{EHI}_t(x) = \mathbb{E}_{F^{(1)}(x), F^{(2)}(x)}[\text{Vol}(\text{Dom}(\boldsymbol{\mu}_t^{(\mathbf{F})}(\mathcal{X}) \cup \{(F^{(1)}(x), F^{(2)}(x))\}; \mathbf{r}_t) \setminus \text{Dom}(\boldsymbol{\mu}_t^{(\mathbf{F})}(\mathcal{X}); \mathbf{r}_t))].$$

Table 3: Computational time (second) and computational time ratio for each setting when  $N_x = 50$  and  $N_w = 100$

	Random	UCB_F1	UCB_F2	MVA	EHI	Proposed
Computational time (Standard error)	0.000 (0.000)	0.181 (0.001)	0.185 (0.001)	0.375 (0.001)	45.77 (0.025)	0.364 (0.001)
Computational time ratio (Standard error)	0.000 (0.000)	0.500 (0.002)	0.510 (0.002)	1.031 (0.003)	126.15 (0.327)	1 (0)

Table 4: Computational time (second) and computational time ratio for each setting when  $N_x = 100$  and  $N_w = 50$

	Random	UCB_F1	UCB_F2	MVA	EHI	Proposed
Computational time (Standard error)	0.000 (0.000)	0.134 (0.001)	0.135 (0.001)	0.272 (0.001)	31.97 (0.015)	0.268 (0.001)
Computational time ratio (Standard error)	0.000 (0.000)	0.503 (0.002)	0.507 (0.002)	1.019 (0.004)	119.92 (0.346)	1 (0)

Table 5: Computational time (second) and computational time ratio for each setting when  $N_x = 100$  and  $N_w = 100$

	Random	UCB_F1	UCB_F2	MVA	EHI	Proposed
Computational time (Standard error)	0.000 (0.000)	0.360 (0.001)	0.362 (0.001)	0.719 (0.002)	91.82 (0.099)	0.726 (0.002)
Computational time ratio (Standard error)	0.000 (0.000)	0.496 (0.001)	0.500 (0.001)	0.991 (0.002)	127.02 (0.412)	1 (0)

Here, for a bounded set  $A$ ,  $\text{Vol}(A)$  represents the hypervolume of  $A$ . Because  $F^{(1)}(x)$  and  $F^{(2)}(x)$  do not follow GPs, we cannot calculate  $\text{EHI}_t(x)$  analytically. Thus, we approximate it by using samples from posterior distributions. Let  $M$  be a number of Monte Carlo sampling, and let  $(f_{t,(l)}^{(j)}(x, w_1), \dots, f_{t,(l)}^{(j)}(x, w_{|\Omega|}))$  be an  $l$ th sample from the posterior distribution of  $(f^{(j)}(x, w_1), \dots, f^{(j)}(x, w_{|\Omega|}))$  at iteration  $t$ , where  $1 \leq l \leq M$ ,  $j \in \{1, 2\}$  and  $x \in \mathcal{X}$ . Then, for each  $t$ , we calculate  $F_{t,(l)}^{(1)}(x)$  and  $F_{t,(l)}^{(2)}(x)$  as

$$F_{t,(l)}^{(1)}(x) = \inf_{p(w) \in \mathcal{A}} \sum_{w \in \Omega} f_{t,(l)}^{(1)}(x, w)p(w), \quad F_{t,(l)}^{(2)}(x) = \inf_{p(w) \in \mathcal{A}} \sum_{w \in \Omega} f_{t,(l)}^{(2)}(x, w)p(w).$$

Using this, we approximate  $\text{EHI}_t(x)$  as

$$\frac{1}{M} \sum_{l=1}^M \text{Vol}(\text{Dom}(\boldsymbol{\mu}_t^{(\mathbf{F})}(\mathcal{X}) \cup \{(F_{t,(l)}^{(1)}(x), F_{t,(l)}^{(2)}(x))\}; \mathbf{r}_t) \setminus \text{Dom}(\boldsymbol{\mu}_t^{(\mathbf{F})}(\mathcal{X}); \mathbf{r}_t)).$$

**Additional Computational Time Experiments** We also compared the computational time of each method by changing input space settings conducted in Section 5.2. In this experiment, the input space  $\mathcal{X} \times \Omega$  was a set of grid points divided into  $[-10, 10] \times [-10, 10]$  equally spaced at  $N_x \times N_w$ . We compared computational times using (50, 100), (100, 50) and (100, 100) as  $(N_x, N_w)$ . From Table 3–5, it can be confirmed that the results are similar to the experimental results conducted in Section 5.2.